Sensitivity of seismic waves to the structure

Luděk Klimeš
Department of Geophysics, Faculty of Mathematics and Physics, Charles University, Ke Karlovu 3, 121 16 Praha 2, Czech Republic, http://sw3d.mff.cuni.cz/staff/klimes.htm

Summary

We study how the perturbations of a generally heterogeneous isotropic or anisotropic structure manifest themselves in the wavefield, and which perturbations can be detected within a limited aperture and a limited frequency band. A short–duration broad–band incident wavefield with a smooth frequency spectrum is considered. Infinitesimally small perturbations of elastic moduli and density are decomposed into Gabor functions. The wavefield scattered by the perturbations is then composed of waves scattered by individual Gabor functions. The scattered waves are estimated using the first–order Born approximation with the paraxial ray approximation.

For each incident wave, each Gabor function generates at most 5 scattered waves, propagating in specific directions. A Gabor function corresponding to a low wavenumber may generate a single broad–band unconverted wave scattered in forward or narrow–angle directions. A Gabor function corresponding to a high wavenumber usually generates 0 to 5 narrow–band Gaussian packets scattered in wide angles, but may also occasionally generate a narrow–band P to S or S to P converted Gaussian packet scattered in a forward direction, or a broad–band S to P (and even S to S in a strongly anisotropic background) converted wave scattered in wide angles.

For a particular source, each wave scattered by a Gabor function at a given spatial location is sensitive to just a single linear combination of 22 values of the elastic moduli and density corresponding to the Gabor function. This information about the Gabor function is lost if the scattered wave does not fall into the aperture covered by the receivers and into the legible frequency band.

The derived approximate solution of the forward scattering problem may be utilized in designing the migration algorithm based on true linearized inversion of the complete set of seismograms recorded for all shots.

Keywords

Elastic waves, elastic moduli, perturbation, Born approximation, paraxial ray approximation, inversion, seismic anisotropy, heterogeneous media.

In: Seismic Waves in Complex 3–D Structures, Report 17 (Department of Geophysics, Charles University, Prague, 2007), pp. 27–61

1. Introduction

We shall study how the perturbations of a generally heterogeneous isotropic or anisotropic structure manifest themselves in the wavefield, and which perturbations can be detected within a limited aperture and a limited frequency band. We consider a smoothly varying heterogeneous generally anisotropic background medium, with an isotropic background medium as a special case. We consider generally anisotropic perturbations of the medium. We first derive the scattered wavefield in the frequency domain and then in the time domain. In the time domain, we assume a short–duration broad–band incident wavefield with a smooth frequency spectrum.

In Section 2, we decompose infinitesimally small perturbations of elastic moduli and density into Gabor functions. The wavefield scattered by the perturbations is then composed of waves scattered by individual Gabor functions. The scattered waves are estimated using the first–order Born approximation with the paraxial ray approximation. These approximations are described in Section 3. Gaussian beams, scattered by individual Gabor functions in the time domain, are derived in Section 4. Gaussian packets, scattered by individual Gabor functions in the time domain, are then derived in Section 5. Sections 6, 7 and 8 are devoted to the discussion of limited aperture, to the application of the derived equations to the linearized inversion of scattered wavefields, and to other remarks on applications.

2. Gabor representation of medium perturbations

We consider infinitesimally small perturbations $\delta c_{ijkl}(\mathbf{x})$ and $\delta\varrho(\mathbf{x})$ of elastic moduli $c_{ijkl}(\mathbf{x})$ and density $\varrho(\mathbf{x})$ in elastodynamic equation

$$\varrho(\mathbf{x})\ \ddot{u}_i(\mathbf{x},t) = [c_{ijkl}(\mathbf{x})\ u_{k,l}(\mathbf{x},t)]_{,j} + f_i(\mathbf{x},t) \quad , \tag{1}$$

where dot $\dot{}$ stands for the derivative with respect to time, and subscript $_{,j}$ following a comma stands for the partial derivative with respect to Cartesian spatial coordinate x_j. Term $f_i(\mathbf{x},t)$ represents the source of the wavefield.

First–order perturbation (variation) δ of elastodynamic equation (1) yields elastodynamic equation

$$\varrho(\mathbf{x})\ \delta\ddot{u}_i(\mathbf{x},t) = [c_{ijkl}(\mathbf{x})\ \delta u_{k,l}(\mathbf{x},t)]_{,j} - \delta\varrho(\mathbf{x})\ \ddot{u}_i(\mathbf{x},t) + [\delta c_{ijkl}(\mathbf{x})\ u_{k,l}(\mathbf{x},t)]_{,j} \tag{2}$$

for wavefield perturbation $\delta u_{k,l}(\mathbf{x},t)$ due to medium perturbation $\delta c_{ijkl}(\mathbf{x})$ and $\delta\varrho(\mathbf{x})$.

The perturbations are decomposed into Gabor functions $g^\alpha(\mathbf{x})$,

$$\delta c_{ijkl}(\mathbf{x}) = \sum_\alpha c^\alpha_{ijkl}\ g^\alpha(\mathbf{x}) \quad , \qquad \delta\varrho(\mathbf{x}) = \sum_\alpha \varrho^\alpha g^\alpha(\mathbf{x}) \quad , \tag{3}$$

where the Gabor functions

$$g^\alpha(\mathbf{x}) = \exp[\mathrm{i}\mathbf{k}^{\alpha\mathrm{T}}(\mathbf{x}-\mathbf{x}^\alpha) - \tfrac{1}{2}(\mathbf{x}-\mathbf{x}^\alpha)^\mathrm{T}\mathbf{K}^\alpha(\mathbf{x}-\mathbf{x}^\alpha)] \tag{4}$$

are centred at various spatial positions $\mathbf{x}^\alpha = (x^\alpha_1, x^\alpha_2, x^\alpha_3)$ and have various structural wavenumber vectors $\mathbf{k}^\alpha = (k^\alpha_1, k^\alpha_2, k^\alpha_3)$. For real–valued perturbations $\delta c_{ijkl}(\mathbf{x})$ of the elastic moduli, we may wish to select matrices $\mathbf{K}^\alpha$ and $\mathbf{K}^\beta$ and coefficients c^α_{ijkl} and c^β_{ijkl} corresponding to $k^\alpha = -k^\beta$ complex–conjugate, $\mathbf{K}^\alpha = (\mathbf{K}^\beta)^*$, $c^\alpha_{ijkl} = (c^\beta_{ijkl})^*$.

The wavefield scattered by the perturbations is then composed of waves $u^\alpha_i(\mathbf{x},t)$ scattered by individual Gabor functions,

$$\delta u_i(\mathbf{x},t) = \sum_\alpha u^\alpha_i(\mathbf{x},t) \quad , \tag{5}$$

see Figures 1, 2, 3.

Figure 1. A single Gabor function $g^\alpha(\mathbf{x})$ at point $\mathbf{x}^\alpha$.

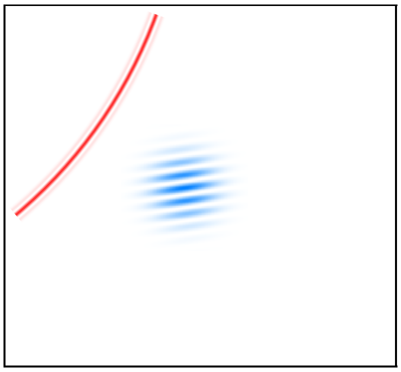

Figure 2. Broad–band wave $u_i(\mathbf{x},t)$ incident at the Gabor function.

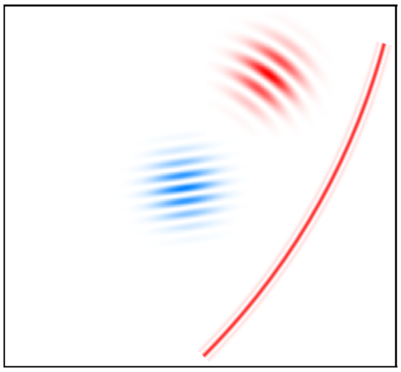

Figure 3. Scattered wave $u_i^\alpha(\mathbf{x},t)$.

3. Applied approximations

3.1. First–order Born approximation

The first–order sensitivity of the wavefield to the infinitesimally small structural perturbations is exactly described by the first–order Born approximation.

The *elastodynamic Green tensor* $G_{km}(\mathbf{x},\mathbf{x}',t)$, corresponding to elastodynamic equation (1), is defined by equation (Červený 2001, eq. 2.5.37)

$$\varrho(\mathbf{x})\,\ddot{G}_{im}(\mathbf{x},\mathbf{x}',t-t') = [c_{ijkl}(\mathbf{x})\;G_{km,l}(\mathbf{x},\mathbf{x}',t-t')]_{,j} + \delta_{im}\,\delta(\mathbf{x}-\mathbf{x}')\,\delta(t-t') \;, \tag{6}$$

where the spatial partial derivatives are related to coordinates x_i. The corresponding time–harmonic elastodynamic Green tensor $\widehat{G}_{km}(\mathbf{x},\mathbf{x}',\omega)$ is defined by equation (Červený 2001, eq. 2.5.38)

$$-\omega^2\,\varrho(\mathbf{x})\;\widehat{G}_{im}(\mathbf{x},\mathbf{x}',\omega) = [c_{ijkl}(\mathbf{x})\;\widehat{G}_{km,l}(\mathbf{x},\mathbf{x}',\omega)]_{,j} + \delta_{im}\,\delta(\mathbf{x}-\mathbf{x}') \quad , \tag{7}$$

where the spatial partial derivatives are again related to coordinates x_i. Multiplying equation (6) by $f_i(\mathbf{x}',t')$, integrating over $\mathbf{x}'$ and t', and comparing the result with (1), we see that

$$u_i(\mathbf{x},t) = \int\!\mathrm{d}\mathbf{x}'\!\int\!\mathrm{d}t'\;G_{im}(\mathbf{x},\mathbf{x}',t-t')f_m(\mathbf{x}',t') \quad . \tag{8}$$

For equation (2), we analogously obtain

$$\delta u_i(\mathbf{x},t) = \int\!\mathrm{d}\mathbf{x}'\!\int\!\mathrm{d}t'\;G_{im}(\mathbf{x},\mathbf{x}',t-t')\,\{-\delta\varrho(\mathbf{x}')\ddot{u}_m(\mathbf{x}',t') + [\delta c_{mjkl}(\mathbf{x}')u_{k,l}(\mathbf{x}',t')]_{,j}\} \;. \tag{9}$$

We define the Fourier transform $\widehat{u}(\omega)$ of function $u(t)$ according to Červený (2001, eq. A.1.2),

$$\widehat{u}(\omega) = \int_{-\infty}^{+\infty}\mathrm{d}t\,\exp(\mathrm{i}\omega t)\,u(t) \quad . \tag{10}$$

The inverse Fourier transformation then reads

$$u(t) = \frac{1}{2\pi}\int_{-\infty}^{+\infty}\mathrm{d}\omega\,\exp(-\mathrm{i}\omega t)\,\widehat{u}(\omega) \quad . \tag{11}$$

If $u(t)$ is a real–valued function, then

$$\widehat{u}(-\omega) = [\widehat{u}(\omega)]^* \quad , \tag{12}$$

and (Červený, 2001, eq. A.1.3)

$$u(t) = \mathrm{Re}[u^{(\mathrm{A})}(t)] \quad , \tag{13}$$

where

$$u^{(\mathrm{A})}(t) = \frac{1}{\pi}\int_0^{+\infty}\mathrm{d}\omega \exp(-\mathrm{i}\omega t)\,\widehat{u}(\omega) \tag{14}$$

is the complex–valued analytical signal corresponding to real–valued function $u(t)$. If we know the analytical signal, we may also use Fourier transform

$$\widehat{u}(\omega) = \tfrac{1}{2}\int_{-\infty}^{+\infty}\mathrm{d}t \exp(\mathrm{i}\omega t)\,u^{(\mathrm{A})}(t) \tag{15}$$

(Červený, 2001, eq. A.3.4) for positive frequencies, and relation (12) for negative frequencies.

In this paper, we shall assume that the frequency is positive,

$$\omega > 0 \quad , \tag{16}$$

and consider Fourier transforms (10) for a real–valued function or (15) for the corresponding analytical signal, and inverse Fourier transform (14).

Fourier transformation (10) of equation (9) yields equation (Červený 2001, eq. 2.6.17)

$$\delta\widehat{u}_i(\mathbf{x},\omega) = \int\mathrm{d}\mathbf{x}'\ \widehat{G}_{im}(\mathbf{x},\mathbf{x}',\omega)\left\{\omega^2\,\delta\varrho(\mathbf{x}')\,\widehat{u}_m(\mathbf{x}',\omega) + [\delta c_{mjkl}(\mathbf{x}')\widehat{u}_{k,l}(\mathbf{x}',\omega)]_{,j}\right\} \ , \tag{17}$$

where $\widehat{u}_{k,l}(\mathbf{x},\omega)$ is the Fourier transform of $u_{k,l}(\mathbf{x},t)$, $\delta\widehat{u}_{k,l}(\mathbf{x},\omega)$ is the Fourier transform of $\delta u_{k,l}(\mathbf{x},t)$, and time–harmonic elastodynamic Green tensor $G_{im}(\mathbf{x},\mathbf{x}',\omega)$ is defined by equation (7).

For the medium perturbation vanishing at the spatial boundary of the integration region, we obtain the first–order wavefield perturbation in the form of the *first–order Born approximation* for the scattered wavefield (Červený 2001, eq. 2.6.18),

$$\begin{aligned}\delta\widehat{u}_i(\mathbf{x},\omega) = \int\mathrm{d}\mathbf{x}'\,\big[\omega^2\,\widehat{G}_{im}(\mathbf{x},\mathbf{x}',\omega)\ \delta\varrho(\mathbf{x}')\ \widehat{u}_m(\mathbf{x}',\omega)&\\ -\widehat{G}_{im,j}(\mathbf{x},\mathbf{x}',\omega)\ \delta c_{mjkl}(\mathbf{x}')\ \widehat{u}_{k,l}(\mathbf{x}',\omega)\big]& \quad ,\end{aligned} \tag{18}$$

where the spatial partial derivatives are related to coordinates x'_i. Inserting equations (3) and (5) for the perturbations, we arrive at equation

$$\begin{aligned}\widehat{u}^{\alpha}_i(\mathbf{x},\omega) = \int\mathrm{d}\mathbf{x}'g^{\alpha}(\mathbf{x}')[\omega^2\,\widehat{G}_{im}(\mathbf{x},\mathbf{x}',\omega)\,\varrho^{\alpha}\,\widehat{u}_m(\mathbf{x}',\omega)&\\ -\widehat{G}_{im,j}(\mathbf{x},\mathbf{x}',\omega)\,c^{\alpha}_{mjkl}\,\widehat{u}_{k,l}(\mathbf{x}',\omega)]& \quad ,\end{aligned} \tag{19}$$

where the spatial partial derivatives are related to coordinates x'_i.

3.2. Ray–theory approximation

The Fourier transform of the incident wave in the vicinity of point $\mathbf{x}^\alpha$ is assumed in form

$$\widehat{u}_i(\mathbf{x}',\omega) \approx \widehat{A}(\mathbf{x}',\omega) E_i(\mathbf{x}') \exp[\mathrm{i}\omega T(\mathbf{x}')] \tag{20}$$

with amplitude $\widehat{A}(\mathbf{x}',\omega)$, polarization vector $E_i(\mathbf{x}')$ and travel time $T(\mathbf{x}')$.

Ray–theory approximation of the time–harmonic elastodynamic Green tensor, corresponding to the elementary wave with polarization vector $e_k(\mathbf{x}',\mathbf{x})$ at point $\mathbf{x}'$ and polarization vector $e_k(\mathbf{x},\mathbf{x}')$ at point $\mathbf{x}$, is (Červený 2001, eq. 5.4.24)

$$\widehat{G}_{im}(\mathbf{x},\mathbf{x}',\omega) \approx \frac{e_i(\mathbf{x},\mathbf{x}')\; e_m(\mathbf{x}',\mathbf{x})\; R(\mathbf{x},\mathbf{x}')}{4\pi\sqrt{\varrho(\mathbf{x})v(\mathbf{x})\varrho(\mathbf{x}')v(\mathbf{x}')}\; L(\mathbf{x},\mathbf{x}')} \; \exp[\mathrm{i}\omega\tau(\mathbf{x},\mathbf{x}')] \quad , \tag{21}$$

where $v(\mathbf{x})$ is the phase velocity, $\varrho(\mathbf{x})$ is the density, and $R(\mathbf{x},\mathbf{x}')$ is the accumulated reciprocal transmission coefficient describing amplitude losses between points $\mathbf{x}'$ and $\mathbf{x}$ due to attenuation and due to reflections and scattering into directions leading outside the vicinity of point $\mathbf{x}$. Here the *relative geometrical spreading* $L(\mathbf{x},\mathbf{x}')$ (Červený 2001, eq. 4.14.45) should correctly include possible phase shifts due to caustics.

3.3. Paraxial ray approximation

Point $\mathbf{x}'$ is situated in the vicinity of point $\mathbf{x}^\alpha$, and observation point $\mathbf{x}$ is situated in the vicinity of point $\mathbf{x}^0$. Point $\mathbf{x}^0$ will be selected in the direction of maximum scattering. We shall apply the *paraxial ray approximation* to both incident wave $u_k(\mathbf{x}',t')$ and Green tensor $G_{im,j}(\mathbf{x},\mathbf{x}',t)$ from point $\mathbf{x}^\alpha$ to point $\mathbf{x}'$. We shall also use the two–point paraxial approximation of Green tensor $G_{im,j}(\mathbf{x},\mathbf{x}',t)$ from point $\mathbf{x}^\alpha$ to point $\mathbf{x}'$ and from point $\mathbf{x}^0$ to point $\mathbf{x}$. The paraxial ray approximation consists in a constant amplitude and in the second–order Taylor expansion of travel time at points $\mathbf{x}^\alpha$ and $\mathbf{x}^0$.

A "constant amplitude" means that we shall apply approximations

$$\widehat{A}(\mathbf{x}',\omega) \approx \widehat{A}(\mathbf{x}^\alpha,\omega) \quad , \tag{22}$$

$$E_i(\mathbf{x}') \approx E_i(\mathbf{x}^\alpha) \quad , \tag{23}$$

$$e_i(\mathbf{x}',\mathbf{x}) \approx e_i(\mathbf{x}^\alpha,\mathbf{x}) \quad , \tag{24}$$

$$e_i(\mathbf{x},\mathbf{x}') \approx e_i(\mathbf{x},\mathbf{x}^\alpha) \quad , \tag{25}$$

$$\varrho(\mathbf{x}') \approx \varrho(\mathbf{x}^\alpha) \quad , \tag{26}$$

$$v(\mathbf{x}') \approx v(\mathbf{x}^\alpha) \quad , \tag{27}$$

$$R(\mathbf{x},\mathbf{x}') \approx R(\mathbf{x},\mathbf{x}^\alpha) \quad , \tag{28}$$

$$\mathbf{Q}_2(\mathbf{x},\mathbf{x}') \approx \mathbf{Q}_2(\mathbf{x},\mathbf{x}^\alpha) \tag{29}$$

in the vicinity of point $\mathbf{x}^\alpha$.

We may also apply approximations

$$e_i(\mathbf{x}^\alpha,\mathbf{x}) \approx e_i(\mathbf{x}^\alpha,\mathbf{x}^0) \quad , \tag{30}$$

$$e_i(\mathbf{x},\mathbf{x}^\alpha) \approx e_i(\mathbf{x}^0,\mathbf{x}^\alpha) \quad , \tag{31}$$

$$\varrho(\mathbf{x}) \approx \varrho(\mathbf{x}^0) \quad , \tag{32}$$

$$v(\mathbf{x}) \approx v(\mathbf{x}^0) \quad , \tag{33}$$

$$R(\mathbf{x},\mathbf{x}^\alpha) \approx R(\mathbf{x}^0,\mathbf{x}^\alpha) \quad , \tag{34}$$

$$\mathbf{Q}_2(\mathbf{x},\mathbf{x}^\alpha) \approx \mathbf{Q}_2(\mathbf{x}^0,\mathbf{x}^\alpha) \tag{35}$$

in the vicinity of point $\mathbf{x}^0$, e.g., in Sections 4.4.3 or 5.3.

For travel time $T(\mathbf{x}')$ of the incident wave at point $\mathbf{x}'$, situated in the vicinity of point $\mathbf{x}^\alpha$, we denote

$$T^\alpha = T(\mathbf{x}^\alpha) \quad , \tag{36}$$

$$T^\alpha_{,i} = \frac{\partial T(\mathbf{x}^\alpha)}{\partial x^\alpha_i} \quad , \tag{37}$$

$$T^\alpha_{,ij} = \frac{\partial^2 T(\mathbf{x}^\alpha)}{\partial x^\alpha_i \partial x^\alpha_j} \quad . \tag{38}$$

The slowness vector of the incident wave at point $\mathbf{x}^\alpha$ is

$$P_i = T^\alpha_{,i} \quad . \tag{39}$$

The second–order Taylor expansion of travel time of the incident wave at point $\mathbf{x}^\alpha$ is

$$T(\mathbf{x}') \approx T^\alpha + P_i \Delta x'_i + \tfrac{1}{2} T^\alpha_{,ij} \Delta x'_i \Delta x'_j \quad , \tag{40}$$

where

$$\Delta x'_i = x'_i - x^\alpha_i \quad . \tag{41}$$

We denote the spatial derivatives of travel time $\tau(\mathbf{x},\mathbf{x}')$ from point $\mathbf{x}'$ to observation point $\mathbf{x}$ as

$$\tau_{,i}(\mathbf{x},\mathbf{x}') = \frac{\partial \tau(\mathbf{x},\mathbf{x}')}{\partial x_i} \quad , \tag{42}$$

$$\tau'_{,i}(\mathbf{x},\mathbf{x}') = \frac{\partial \tau(\mathbf{x},\mathbf{x}')}{\partial x'_i} \quad , \tag{43}$$

$$\tau_{,ij}(\mathbf{x},\mathbf{x}') = \frac{\partial^2 \tau(\mathbf{x},\mathbf{x}')}{\partial x_i \partial x_j} \quad , \tag{44}$$

$$\tau'_{,ij}(\mathbf{x},\mathbf{x}') = \frac{\partial^2 \tau(\mathbf{x},\mathbf{x}')}{\partial x_i \partial x'_j} \quad , \tag{45}$$

$$\tau''_{,ij}(\mathbf{x},\mathbf{x}') = \frac{\partial^2 \tau(\mathbf{x},\mathbf{x}')}{\partial x'_i \partial x'_j} \quad . \tag{46}$$

At point $\mathbf{x}^\alpha$, we denote

$$\tau^\alpha(\mathbf{x}) = \tau(\mathbf{x},\mathbf{x}^\alpha) \quad , \tag{47}$$

$$\tau^{\alpha\prime}_{,i}(\mathbf{x}) = \tau'_{,i}(\mathbf{x},\mathbf{x}^\alpha) \quad , \tag{48}$$

$$\tau^{\alpha\prime\prime}_{,ij}(\mathbf{x}) = \tau''_{,ij}(\mathbf{x},\mathbf{x}^\alpha) \quad . \tag{49}$$

Slowness vector at point $\mathbf{x}^\alpha$ pointing towards observation point $\mathbf{x}$ is

$$p_i(\mathbf{x}) = -\tau^{\alpha\prime}_{,i}(\mathbf{x}) \quad . \tag{50}$$

The second–order Taylor expansion of travel time $\tau(\mathbf{x},\mathbf{x}')$ at point $\mathbf{x}^\alpha$ is

$$\tau(\mathbf{x},\mathbf{x}') \approx \tau^\alpha(\mathbf{x}) + \tau^{\alpha\prime}_{,i}(\mathbf{x})\Delta x'_i + \tfrac{1}{2}\tau^{\alpha\prime\prime}_{,ij}(\mathbf{x})\Delta x'_i \Delta x'_j \quad , \tag{51}$$

or, in terms of the slowness vector,

$$\tau(\mathbf{x},\mathbf{x}') \approx \tau^\alpha(\mathbf{x}) - p_i(\mathbf{x})\Delta x'_i + \tfrac{1}{2}\tau^{\alpha\prime\prime}_{,ij}(\mathbf{x})\Delta x'_i \Delta x'_j \quad . \tag{52}$$

At point $\mathbf{x}^0$, we denote

$$\tau^0 = \tau(\mathbf{x}^0, \mathbf{x}^\alpha) \quad , \tag{53}$$

$$\tau^0_{,i} = \tau_{,i}(\mathbf{x}^0, \mathbf{x}^\alpha) \quad , \tag{54}$$

$$\tau^{0\prime}_{,i} = \tau'_{,i}(\mathbf{x}^0, \mathbf{x}^\alpha) \quad , \tag{55}$$

$$\tau^0_{,ij} = \tau_{,ij}(\mathbf{x}^0, \mathbf{x}^\alpha) \quad , \tag{56}$$

$$\tau^{0\prime}_{,ij} = \tau'_{,ij}(\mathbf{x}^0, \mathbf{x}^\alpha) \quad , \tag{57}$$

$$\tau^{0\prime\prime}_{,ij} = \tau''_{,ij}(\mathbf{x}^0, \mathbf{x}^\alpha) \quad . \tag{58}$$

Slowness vector at point $\mathbf{x}^\alpha$ pointing towards point $\mathbf{x}^0$ is

$$p^0_i = p_i(\mathbf{x}^0) = -\tau^{0\prime}_{,i} \quad . \tag{59}$$

The second–order Taylor expansion of travel time (47) at point $\mathbf{x}^0$ is

$$\tau^\alpha(\mathbf{x}) \approx \tau^0 + \tau^0_{,i}\Delta x_i + \tfrac{1}{2}\tau^0_{,ij}\Delta x_i \Delta x_j \quad , \tag{60}$$

where

$$\Delta x_i = x_i - x^0_i \quad . \tag{61}$$

The corresponding Taylor expansions of travel time derivatives (48) and (49) at point $\mathbf{x}^0$ are

$$\tau^{\alpha\prime}_{,i}(\mathbf{x}) \approx \tau^{0\prime}_{,i} + \tau^{0\prime}_{,ji}\Delta x_j \quad , \tag{62}$$

$$\tau^{\alpha\prime\prime}_{,ij}(\mathbf{x}) \approx \tau^{0\prime\prime}_{,ij} \quad . \tag{63}$$

3.4. High–frequency approximation of spatial derivatives

We use the *high–frequency approximation of spatial derivatives,*

$$u_{i,k}(\mathbf{x}', t) \approx -\dot{u}_i(\mathbf{x}', t)\; P_k \quad , \qquad \frac{\partial G_{ij}}{\partial x'_k}(\mathbf{x}, \mathbf{x}', t) \approx \dot{G}_{ij}(\mathbf{x}, \mathbf{x}', t)\; p_k(\mathbf{x}) \quad , \tag{64}$$

and

$$\widehat{u}_{i,k}(\mathbf{x}', \omega) \approx \mathrm{i}\omega\, \widehat{u}_i(\mathbf{x}', \omega)\; P_k \quad , \qquad \frac{\partial \widehat{G}_{ij}}{\partial x'_k}(\mathbf{x}, \mathbf{x}', \omega) \approx -\mathrm{i}\omega\, \widehat{G}_{ij}(\mathbf{x}, \mathbf{x}', \omega)\; p_k(\mathbf{x}) \quad , \tag{65}$$

where P_i defined by (39) is the slowness vector of the incident wave, and $p_k(\mathbf{x})$ defined by (50) is the slowness vector determining the ray leading from point $\mathbf{x}^\alpha$ to point $\mathbf{x}$.

4. Scattering in the frequency domain — Gaussian beams

A *broad–band incident wavefield* (20) having a *smooth frequency spectrum* is considered, with a frequency band limited by the minimum frequency and the maximum frequency.

4.1. Born approximation with paraxial ray approximation at point $\mathbf{x}^\alpha$

Inserting approximations (20)–(29) and (65) into the Born approximation (19), we arrive at

$$\widehat{u}_i^\alpha(\mathbf{x},\omega) = \frac{\omega^2}{2\pi} \frac{e_i(\mathbf{x},\mathbf{x}^\alpha)\; R(\mathbf{x},\mathbf{x}^\alpha)\; \widehat{A}(\mathbf{x}^\alpha,\omega)\; \sqrt{\varrho(\mathbf{x}^\alpha)}}{\sqrt{\varrho(\mathbf{x})v(\mathbf{x})v(\mathbf{x}^\alpha)}L(\mathbf{x},\mathbf{x}^\alpha)}\; r^\alpha(\mathbf{x})\; I^\alpha(\mathbf{x}) \quad , \tag{66}$$

where integral

$$I^\alpha(\mathbf{x}) = \int \mathrm{d}\mathbf{x}'g^\alpha(\mathbf{x}')\; \exp\{\mathrm{i}\omega[T(\mathbf{x}') + \tau(\mathbf{x},\mathbf{x}')]\tag{67}$$

accounts for the directional properties of scattered time–harmonic wave $\widehat{u}_i^\alpha(\mathbf{x},\omega)$.

Here $r^\alpha(\mathbf{x})$ is the “reflectivity function”,

$$\boxed{r^\alpha(\mathbf{x}) = \frac{\varrho^\alpha E_m(\mathbf{x}^\alpha)e_m(\mathbf{x}^\alpha,\mathbf{x}) - c^\alpha_{ijkl}E_i(\mathbf{x}^\alpha)P_j e_k(\mathbf{x}^\alpha,\mathbf{x})p_l(\mathbf{x})}{2\;\varrho(\mathbf{x}^\alpha)} \quad , \qquad (68)}$$

where P_i and E_i are the slowness vector and the polarization vector of the incident wave, p_i and e_i are the slowness vector and the polarization vector of the wave scattered at point $\mathbf{x}^\alpha$ and propagating towards point $\mathbf{x}$. Density $\varrho = \varrho(\mathbf{x}^\alpha)$ corresponds to the background.

We now introduce travel time

$$\theta(\mathbf{x},\mathbf{x}') = \tau(\mathbf{x},\mathbf{x}') + T(\mathbf{x}') \tag{69}$$

through point $\mathbf{x}'$ to observation point $\mathbf{x}$, and its second–order Taylor expansion

$$\theta(\mathbf{x},\mathbf{x}') \approx \theta^\alpha(\mathbf{x}) + \theta^{\alpha\prime}_{,i}(\mathbf{x})\Delta x'_i + \tfrac{1}{2}\theta^{\alpha\prime\prime}_{,ij}(\mathbf{x})\Delta x'_i\Delta x'_j \quad , \tag{70}$$

where

$$\theta^\alpha(\mathbf{x}) = T^\alpha + \tau^\alpha(\mathbf{x}) \quad , \tag{71}$$

$$\theta^{\alpha\prime}_{,i}(\mathbf{x}) = T^\alpha_{,i} + \tau^{\alpha\prime}_{,i}(\mathbf{x}) \quad , \tag{72}$$

$$\theta^{\alpha\prime\prime}_{,ij}(\mathbf{x}) = T^\alpha_{,ij} + \tau^{\alpha\prime\prime}_{,ij}(\mathbf{x}) \quad , \tag{73}$$

see (36)–(38) and (47)–(49). Equation (72) may also be expressed in form

$$\theta^{\alpha\prime}_{,i}(\mathbf{x}) = P_i - p_i(\mathbf{x}) \quad , \tag{74}$$

see equations (39) and (50).

Integral (67) with (4) and (70) reads

$$I^\alpha \approx \int \mathrm{d}\Delta\mathbf{x}' \exp\left[\mathrm{i}k^\alpha_i\,\Delta x'_i - \tfrac{1}{2}K^\alpha_{ij}\Delta x'_i\Delta x'_j + \mathrm{i}\omega(\theta^\alpha + \theta^{\alpha\prime}_{,i}\Delta x'_i + \tfrac{1}{2}\theta^{\alpha\prime\prime}_{,ij}\Delta x'_i\Delta x'_j)\right] \; . \tag{75}$$

We rearrange the exponent of the integrand,

$$\begin{aligned} I^\alpha \approx \int \mathrm{d}\Delta\mathbf{x}' \exp\Big\{ & \mathrm{i}\omega\theta^\alpha - \tfrac{1}{2}(K^\alpha_{ij} - \mathrm{i}\omega\theta^{\alpha\prime\prime}_{,ij})[\Delta x'_i - \mathrm{i}(K^\alpha - \mathrm{i}\omega\theta^{\alpha\prime\prime})^{-1}_{ik}(k^\alpha_k + \omega\theta^{\alpha\prime}_{,k})] \\ & \times[\Delta x'_j - \mathrm{i}(K^\alpha - \mathrm{i}\omega\theta^{\alpha\prime\prime})^{-1}_{jl}(k^\alpha_l + \omega\theta^{\alpha\prime}_{,l})] \\ & - \tfrac{1}{2}(K^\alpha - \mathrm{i}\omega\theta^{\alpha\prime\prime})^{-1}_{ij}[k^\alpha_i + \omega\theta^{\alpha\prime}_{,i}][k^\alpha_j + \omega\theta^{\alpha\prime}_{,j}]\Big\} \quad , \end{aligned} \tag{76}$$

where $(K^\alpha - \mathrm{i}\omega\theta^{\alpha\prime\prime})^{-1}_{ij}$ stands for the components of the matrix inverse to matrix $K^\alpha_{ij} - \mathrm{i}\omega\theta^{\alpha\prime\prime}_{,ij}$. We now integrate (76) and arrive at

$$I^\alpha \approx \sqrt{\frac{(2\pi)^3}{\det(K^\alpha_{ij} - \mathrm{i}\omega\theta^{\alpha\prime\prime}_{,ij})}}\ \exp\Big\{\mathrm{i}\omega\theta^\alpha - \tfrac{1}{2}(K^\alpha - \mathrm{i}\omega\theta^{\alpha\prime\prime})^{-1}_{ij}[k^\alpha_i + \omega\theta^{\alpha\prime}_{,i}][k^\alpha_j + \omega\theta^{\alpha\prime}_{,j}]\Big\}\ . \quad (77)$$

In this paper, the square root of the determinant of a symmetric complex–valued matrix is defined as the product of the square roots of its eigenvalues. The square root of each eigenvalue is taken with the positive real part.

Insertion of (77) into (66) yields

$$\boxed{\widehat{u}^\alpha_i(\mathbf{x},\omega) = e_i(\mathbf{x},\mathbf{x}^\alpha)\ \widehat{a}(\mathbf{x},\omega)\ \exp[\mathrm{i}\omega T^\alpha_\omega(\mathbf{x})] \quad , \qquad (78)}$$

where

$$\widehat{a}(\mathbf{x},\omega) = R(\mathbf{x},\mathbf{x}^\alpha)\sqrt{\frac{\varrho(\mathbf{x}^\alpha)v(\mathbf{x}^\alpha)}{\varrho(\mathbf{x})v(\mathbf{x})}}\ \frac{\omega^2\widehat{A}(\mathbf{x}^\alpha,\omega)\ r^\alpha(\mathbf{x})}{v(\mathbf{x}^\alpha)L(\mathbf{x},\mathbf{x}^\alpha)}\ \frac{\sqrt{2\pi}}{\sqrt{\det(K^\alpha_{ij} - \mathrm{i}\omega\theta^{\alpha\prime\prime}_{,ij})}} \quad , \qquad (79)$$

and

$$\mathrm{i}\omega T^\alpha_\omega(\mathbf{x}) = \mathrm{i}\omega\theta^\alpha(\mathbf{x}) - \tfrac{1}{2}[K^\alpha - \mathrm{i}\omega\theta^{\alpha\prime\prime}(\mathbf{x})]^{-1}_{ij}[k^\alpha_i + \omega\theta^{\alpha\prime}_{,i}(\mathbf{x})][k^\alpha_j + \omega\theta^{\alpha\prime}_{,j}(\mathbf{x})] \quad . \qquad (80)$$

For given frequency ω and given slowness vector $p_i(\mathbf{x})$, Gabor function $g^\alpha(\mathbf{x}')$ concentrated at point $\mathbf{x}^\alpha$ influence the seismogram for structural wavenumbers from the vicinity of the "wavenumber surface" parametrized by $p_i(\mathbf{x})$ and defined by equation

$$k^\alpha_i = -\omega\theta^{\alpha\prime}_{,i}(\mathbf{x}) = \omega\,[p_i(\mathbf{x}) - P_i] \quad . \qquad (81)$$

For illustration, refer to transform (209) and to Figures 4, 5 and 6.

4.2. Paraxial ray approximation at point $\mathbf{x}^0$

Inserting Taylor expansions (60), (62) and (63) into definitions (71), (72) and (73), we obtain Taylor expansions

$$\theta^\alpha(\mathbf{x}) = T^\alpha + \tau^0 + \tau^0_{,i}\Delta x_i + \tfrac{1}{2}\tau^0_{,ij}\Delta x_i\Delta x_j \quad , \qquad (82)$$

$$\theta^{\alpha\prime}_{,i}(\mathbf{x}) = T^\alpha_{,i} + \tau^{0\prime}_{,i} + \tau^{0\prime}_{,ji}\Delta x_j \quad , \qquad (83)$$

$$\theta^{\alpha\prime\prime}_{,ij}(\mathbf{x}) = \theta^{0\prime\prime}_{,ij} \quad , \qquad (84)$$

where

$$\theta^{0\prime\prime}_{,ij} = T^\alpha_{,ij} + \tau^{0\prime\prime}_{,ij} \quad . \qquad (85)$$

The Taylor expansion of (80) in the vicinity of point $\mathbf{x}^0$ then reads

$$\mathrm{i}\omega T^\alpha_\omega(\mathbf{x}) = \mathrm{i}\omega[T^\alpha + \tau^0 + \tau^0_{,i}\Delta x_i + \tfrac{1}{2}\tau^0_{,ij}\Delta x_i\Delta x_j]$$
$$-\tfrac{1}{2}(K^\alpha - \mathrm{i}\omega\theta^{0\prime\prime})^{-1}_{ij}[k^\alpha_i + \omega(T^\alpha_{,i} + \tau^{0\prime}_{,i} + \tau^{0\prime}_{,mi}\Delta x_m)][k^\alpha_j + \omega(T^\alpha_{,j} + \tau^{0\prime}_{,j} + \tau^{0\prime}_{,nj}\Delta x_n)]\ . \quad (86)$$

Since the real part of matrix $(K^\alpha - \mathrm{i}\omega\theta^{0\prime\prime})^{-1}_{ij}$ is positive–definite, the maximum scattering (extreme of real part of $\mathrm{i}\omega T^\alpha_\omega(\mathbf{x})$) at the axial ray $\Delta x = 0$ occurs if

$$k^\alpha_i + \omega\,(T^\alpha_{,i} + \tau^{0\prime}_{,i}) = 0 \quad , \qquad (87)$$

i.e., if

$$p^0_i = P_i + \omega^{-1}k^\alpha_i \quad , \qquad (88)$$

see equations (39) and (59). Inserting (88) into existence condition (Červený 2001, eq. 2.2.36)

$$\det[c_{ijkl}(\mathbf{x}^\alpha)p_j^0p_l^0 - \varrho(\mathbf{x}^\alpha)\delta_{ik}] = 0 \quad , \tag{89}$$

we obtain the sixth–order polynomial equation

$$\det\{c_{ijkl}(\mathbf{x}^\alpha)[P_i + (\omega^0)^{-1}k_i^\alpha][P_l + (\omega^0)^{-1}k_l^\alpha] - \varrho(\mathbf{x}^\alpha)\delta_{ik}\} = 0 \tag{90}$$

for frequencies $\omega = \omega^0$ corresponding to maximum scattering by Gabor function $g^\alpha(\mathbf{x})$. Because slowness vector P_i of the incident wave satisfies the characteristic equation, equation (90) has a trivial solution $(\omega^0)^{-1} = 0$ corresponding to the forward broad–band scattering. The zero to five *positive* solutions of equation (90) correspond to wide–angle scattering.

For positive ω^0 satisfying equation (90), we choose

$$\boxed{p_i^0 = P_i + (\omega^0)^{-1}k_i^\alpha \quad .} \tag{91}$$

We assume that point $\mathbf{x}^0$ is situated on the ray determined by initial slowness vector p_i^0, see (59). Then

$$k_i^\alpha + \omega(T_{,i}^\alpha + \tau_{,i}^{0\prime} + \tau_{,mi}^{0\prime}\Delta x_m) = \omega\tau_{,mi}^{0\prime}\Delta x_m - \frac{\Delta\omega}{\omega^0}k_i^\alpha \quad , \tag{92}$$

where

$$\Delta\omega = \omega - \omega^0 \quad . \tag{93}$$

We insert (92) into (86),

$$\begin{aligned} T_\omega^\alpha(\mathbf{x}) =& T^\alpha + \tau^0 + \tau_{,i}^0\Delta x_i + \tfrac{1}{2}\tau_{,ij}^0\Delta x_i\Delta x_j \\ & - \tfrac{1}{2}(\theta^{0\prime\prime} + \mathrm{i}\omega^{-1}K^\alpha)_{ij}^{-1}[\tau_{,mi}^{0\prime}\Delta x_m - \frac{\Delta\omega}{\omega^0\omega}k_i^\alpha][\tau_{,nj}^{0\prime}\Delta x_n - \frac{\Delta\omega}{\omega^0\omega}k_j^\alpha] \quad . \end{aligned} \tag{94}$$

For $\omega = \omega^0$ equation (94) yields

$$T_{\omega^0}^\alpha(\mathbf{x}) = T^\alpha + \tau^0 + \tau_{,i}^0\Delta x_i + \tfrac{1}{2}[\tau_{,ij}^0 - \tau_{,ir}^{0\prime}(\theta^{0\prime\prime} + \mathrm{i}\omega^{-1}K^\alpha)_{rs}^{-1}\tau_{,js}^{0\prime}]\Delta x_i\Delta x_j \quad . \tag{95}$$

Equation (94) then reads

$$T_\omega^\alpha(\mathbf{x}) = T_{\omega^0}^\alpha(\mathbf{x}) + \tau_{,ir}^{0\prime}(\theta^{0\prime\prime} + \mathrm{i}\omega^{-1}K^\alpha)_{rs}^{-1}k_s^\alpha\Delta x_i\frac{\Delta\omega}{\omega^0\omega} - \frac{1}{2}k_r^\alpha(\theta^{0\prime\prime} + \mathrm{i}\omega^{-1}K^\alpha)_{rs}^{-1}k_s^\alpha\left(\frac{\Delta\omega}{\omega^0\omega}\right)^2 . \tag{96}$$

Equation (95) represents the paraxial expansion of the complex–valued travel–time of the time–harmonic Gaussian beam scattered by Gabor function $g^\alpha(\mathbf{x})$ at frequency ω^0. Equation (96) describes the approximate frequency dependence of the scattered Gaussian beam.

To derive the explicit evolution equations with corresponding initial conditions for scattered Gaussian beam (78) with amplitude (79) and travel time (96), we transform all quantities into the ray–centered coordinates attached to the ray leading from point $\mathbf{x}^\alpha$ to point $\mathbf{x}^0$.

4.3. Ray–centred coordinate system

The q_3–coordinate line of ray–centred coordinates q_m is the axial ray parametrized by any parameter q_3 increasing along the axial ray. The Cartesian coordinates corresponding to q_m are

$$x_i = x_i^{\mathrm{R}}(q_3) + h_M^i(q_3)\, q_M \quad , \tag{97}$$

where $x_i^{\mathrm{R}}(q_3)$ are points of the axial ray. This is both the definition of the ray–centred coordinates, and the transformation equation from the ray–centred to Cartesian coordinates. The transformation matrices, taken at the central ray, are

$$h_m^i = \frac{\partial x_i}{\partial q_m} \quad , \qquad \widehat{h}_i^m = \frac{\partial q_m}{\partial x_i} \quad . \tag{98}$$

The "contravariant basis vectors" h_1^i, h_2^i, h_3^i and the "covariant basis vectors" $\widehat{h}_i^1$, $\widehat{h}_i^2$, $\widehat{h}_i^3$ of the ray–centred coordinate system are defined by equations

$$h_3^i = H^{,i} \frac{\mathrm{d}\tau}{\mathrm{d}q_3} \quad , \tag{99}$$

$$\widehat{h}_i^3 = p_i \frac{\mathrm{d}q_3}{\mathrm{d}\tau} \quad , \tag{100}$$

$$h_a^i \widehat{h}_i^b = \delta_a^b \quad . \tag{101}$$

Here

$$H_{,i} = \frac{\partial H}{\partial x_i} \quad , \qquad H^{,i} = \frac{\partial H}{\partial p_i} \tag{102}$$

are the phase–space derivatives of Hamiltonian $H = H(x_m, p_n)$ corresponding to the Gaussian beam scattered at point $\mathbf{x}^\alpha$. We assume in this paper that the Hamiltonian is a homogeneous function of an arbitrary degree with respect to the slowness vector. Then $H^{,i}$ is the ray–velocity vector.

The first two contravariant basis vectors h_1^i, h_2^i of the ray–centred coordinate system are tangent to the wavefront, the third contravariant basis vector h_3^i is tangent to the ray. The first two covariant basis vectors $\widehat{h}_i^1$, $\widehat{h}_i^2$ of the ray–centred coordinate system are perpendicular to the ray, the third covariant basis vector $\widehat{h}_i^3$ is perpendicular to the wavefront. Whereas basis vectors h_3^i and $\widehat{h}_i^3$ are uniquely determined by equations (99) and (100), we may either choose the contravariant basis vectors h_1^i and h_2^i arbitrarily in the wavefront tangent plane, or choose the covariant basis vectors $\widehat{h}_i^1$ and $\widehat{h}_i^2$ arbitrarily in the plane perpendicular to the ray velocity vector h_3^i.

We define the Jacobian

$$h = \det(h_m^i) \tag{103}$$

of the transformation from ray–centred coordinates q_m to Cartesian coordinates x_i. We shall use notation

$$\mathbf{q} = \begin{pmatrix} q_1 \\ q_2 \end{pmatrix} \tag{104}$$

for the first two ray–centred coordinates, and

$$\mathbf{p}^{(q)} = \begin{pmatrix} p_1^{(q)} \\ p_2^{(q)} \end{pmatrix} \tag{105}$$

for the first two ray–centred components

$$p_K^{(q)} = h_K^i p_i \tag{106}$$

of the slowness vector.

4.3.1. Paraxial–ray propagator matrix and the second derivatives of two–point travel time

Differentiating the eikonal equation (stationary Hamilton–Jacobi equation)

$$H(x_m, \tau_{,n}) = 0 \tag{107}$$

with respect to x_i, we obtain

$$H_{,i} + H^{,k}\tau_{,ki} = 0 \quad . \tag{108}$$

Multiplying (108) by $h_a^i \frac{\mathrm{d}\tau}{\mathrm{d}q_3}$ and considering (99), we arrive at expression

$$h_a^i \tau_{,ij} h_3^j = -h_a^i H_{,i} \, \frac{\mathrm{d}\tau}{\mathrm{d}q_3} \tag{109}$$

for the second travel–time derivatives in the ray–centred coordinates. We denote by

$$\begin{pmatrix} \mathbf{M}_3^\alpha \\ M_{33}^\alpha \end{pmatrix} \quad , \qquad \begin{pmatrix} \mathbf{M}_3 \\ M_{33} \end{pmatrix} \tag{110}$$

the right–hand sides of equation (109) at points $\mathbf{x}^\alpha$ and $\mathbf{x}^0$, respectively,

$$M_{a3}^\alpha = -h_a^i(\mathbf{x}^\alpha) H_{,i}(\mathbf{x}^\alpha, -\tau_k^{0\prime}) \, \frac{\mathrm{d}\tau}{\mathrm{d}q_3}(\mathbf{x}^\alpha) \quad , \tag{111}$$

$$M_{a3} = -h_a^i(\mathbf{x}^0) H_{,i}(\mathbf{x}^0, \tau_k^0) \, \frac{\mathrm{d}\tau}{\mathrm{d}q_3}(\mathbf{x}^0) \quad . \tag{112}$$

Note that in an isotropic medium, (111) and (112) are the slowness gradients.

Denote by $\mathbf{Q_1}$, $\mathbf{Q_2}$, $\mathbf{P_1}$ and $\mathbf{P_2}$ the 2×2 submatrices of the 4×4 paraxial ray propagator matrix

$$\mathbf{\Pi}(\mathbf{x}^0, \mathbf{x}^\alpha) = \begin{pmatrix} \mathbf{Q_1} & \mathbf{Q_2} \\ \mathbf{P_1} & \mathbf{P_2} \end{pmatrix} \tag{113}$$

from point $\mathbf{x}^\alpha$ to point $\mathbf{x}^0$ in ray–centred coordinates.

The matrices $\tau_{,ij}^{0\prime\prime}$, $\tau_{,ij}^{0\prime}$, $\tau_{,ij}^0$, covariantly transformed into the ray–centred coordinate system,

$$\tau_{;ab}^{0\prime\prime(q)} = h_a^i(\mathbf{x}^\alpha) \, \tau_{,ij}^{0\prime\prime} \, h_b^j(\mathbf{x}^\alpha) \quad , \tag{114}$$

$$\tau_{;ab}^{0\prime(q)} = h_a^i(\mathbf{x}^0) \, \tau_{,ij}^{0\prime} \, h_b^j(\mathbf{x}^\alpha) \quad , \tag{115}$$

$$\tau_{;ab}^{0(q)} = h_a^i(\mathbf{x}^0) \, \tau_{,ij}^{0} \, h_b^j(\mathbf{x}^0) \quad , \tag{116}$$

represent the second covariant derivatives of travel time in ray–centred coordinates. This means that they represent the partial derivatives of travel time with respect to local Cartesian coordinates

$$\Delta x_m^{(q)\prime} = \widehat{h}_i^m(\mathbf{x}^\alpha) \, \Delta x_i' = \widehat{h}_i^m(\mathbf{x}^\alpha) \, [x_i' - x_i^\alpha] \tag{117}$$

and

$$\Delta x_m^{(q)} = \widehat{h}_i^m(\mathbf{x}^0) \, \Delta x_i = \widehat{h}_i^m(\mathbf{x}^0) \, [x_i - x_i^0] \quad . \tag{118}$$

The matrices $\tau^{0\prime\prime(q)}_{;ab}$ $\tau^{0\prime(q)}_{;ab}$ and $\tau^{0(q)}_{;ab}$ read (Červený, Klimeš & Pšenčík, 1984, eq. 22)

$$\begin{pmatrix} \mathbf{Q_2}^{-1}\mathbf{Q_1} & -\mathbf{M}^\alpha_3 \\ -\mathbf{M}^{\alpha\,\mathrm{T}}_3 & -M^\alpha_{33} \end{pmatrix} \quad , \tag{119}$$

$$\begin{pmatrix} -\mathbf{Q_2}^{-1\,\mathrm{T}} & \mathbf{0} \\ \mathbf{0}^\mathrm{T} & 0 \end{pmatrix} \tag{120}$$

and

$$\begin{pmatrix} \mathbf{P_2}\mathbf{Q_2}^{-1} & \mathbf{M}_3 \\ \mathbf{M}_3^{\mathrm{T}} & M_{33} \end{pmatrix} \quad , \tag{121}$$

respectively.

Note that the matrices $\tau^{0\prime\prime(q)}_{,ab}$ $\tau^{0\prime(q)}_{,ab}$ and $\tau^{0(q)}_{,ab}$ of the second partial derivatives of travel time in ray–centred coordinates have the form analogous to (119), (120) and (121), but with zero $\mathbf{M}^\alpha_3$ and $\mathbf{M}_3$.

4.3.2. Other matrices and vectors appearing in equations (95) and (96)

Denote by

$$\begin{pmatrix} \mathbf{T}^{(q)} & \mathbf{T}^{(q)}_3 \\ \mathbf{T}^{(q)\,\mathrm{T}}_3 & T^{(q)}_{;33} \end{pmatrix} \tag{122}$$

matrix $T^\alpha_{,ij}$ in the ray–centred coordinate system,

$$T^{(q)}_{;ab} = h^i_a(\mathbf{x}^\alpha)\, T^\alpha_{,ij}\, h^j_b(\mathbf{x}^\alpha) \quad , \tag{123}$$

and by

$$\begin{pmatrix} \mathbf{K}^{(q)} & \mathbf{K}^{(q)}_3 \\ \mathbf{K}^{(q)\,\mathrm{T}}_3 & K^{(q)}_{33} \end{pmatrix} \tag{124}$$

matrix K^α_{ij} in the ray–centred coordinate system,

$$K^{(q)}_{ab} = h^i_a(\mathbf{x}^\alpha)\, K^\alpha_{ij}\, h^j_b(\mathbf{x}^\alpha) \quad . \tag{125}$$

Then matrix $\theta^{0\prime\prime}_{,kl}+\mathrm{i}\omega^{-1}K^\alpha_{ij}$, covariantly transformed into the ray–centred coordinate system, is

$$\begin{pmatrix} \mathbf{T}^{(q)} + \mathbf{Q_2}^{-1}\mathbf{Q_1} + \mathrm{i}\omega^{-1}\mathbf{K}^{(q)} & \mathbf{m} \\ \mathbf{m}^\mathrm{T} & m \end{pmatrix} \quad , \tag{126}$$

where

$$\mathbf{m} = \mathbf{T}^{(q)}_3 - \mathbf{M}^\alpha_3 + \mathrm{i}\omega^{-1}\mathbf{K}^{(q)}_3 \tag{127}$$

and

$$m = T^{(q)}_{;33} - M^\alpha_{33} + \mathrm{i}\omega^{-1}K^{(q)}_{33} \quad . \tag{128}$$

Inverse matrix $(\theta^{0\prime\prime} + \mathrm{i}\omega^{-1}K^\alpha)^{-1}_{kl}$, also expressed in the ray–centred coordinate system, is

$$\begin{pmatrix} [\mathbf{Q_2}^{-1}\mathbf{Q_1} + \mathbf{M}^\alpha]^{-1} & -\frac{[\mathbf{Q_2}^{-1}\mathbf{Q_1}+\mathbf{M}^\alpha]^{-1}\mathbf{m}}{m} \\ -\frac{\mathbf{m}^\mathrm{T}[\mathbf{Q_2}^{-1}\mathbf{Q_1}+\mathbf{M}^\alpha]^{-1}}{m} & \frac{1}{m} + \frac{\mathbf{m}^\mathrm{T}[\mathbf{Q_2}^{-1}\mathbf{Q_1}+\mathbf{M}^\alpha]^{-1}\mathbf{m}}{m^2} \end{pmatrix} \quad , \tag{129}$$

where

$$\boxed{\mathbf{M}^\alpha = \mathbf{T}^{(q)} + \mathrm{i}\omega^{-1}\mathbf{K}^{(q)} - \frac{\mathbf{m}\,\mathbf{m}^\mathrm{T}}{m} \quad . \qquad (130)}$$

We shall see later that matrix $\mathbf{M}^\alpha$ describes the initial conditions for the scattered Gaussian beam at point $\mathbf{x}^\alpha$.

We also denote by

$$\begin{pmatrix} \mathbf{k}^{(q)} \\ k_3^{(q)} \end{pmatrix} \tag{131}$$

vector k_i^α covariantly transformed into the ray–centred coordinate system,

$$k_a^{(q)} = h_a^i k_i^\alpha \quad . \tag{132}$$

4.4. Gaussian beams

4.4.1. Complex–valued travel time of the Gaussian beam at frequency ω^0

We denote by

$$\begin{pmatrix} \mathbf{M} & \mathbf{M}_3 \\ \mathbf{M}_3{}^{\mathrm{T}} & M_{33} \end{pmatrix} \tag{133}$$

matrix $\tau^0_{,ij} - \tau^{0\prime}_{,ik}(\theta^{0\prime\prime} + \mathrm{i}\omega^{-1}K^\alpha)^{-1}_{kl}\tau^{0\prime}_{,jl}$ in (95) covariantly transformed into the ray–centred coordinate system,

$$M_{ab} = h_a^i(\mathbf{x}^0)\,[\tau^0_{,ij} - \tau^{0\prime}_{,ik}(\theta^{0\prime\prime} + \mathrm{i}\omega^{-1}K^\alpha)^{-1}_{kl}\tau^{0\prime}_{,jl}]\,h_b^j(\mathbf{x}^0) \quad . \tag{134}$$

Matrix (133) can simply be calculated using matrices (120), (121) and (129). Its submatrices $\mathbf{M}_3$ and M_{33} come directly from (121), and are defined by (110) with (112). The 2×2 submatrix reads

$$\mathbf{M} = \mathbf{P_2Q_2}^{-1} - \mathbf{Q_2}^{-1\,\mathrm{T}}[\mathbf{Q_2}^{-1}\mathbf{Q_1} + \mathbf{M}^\alpha]^{-1}\mathbf{Q_2}^{-1} \quad . \tag{135}$$

Considering the symmetry of $\mathbf{P_2Q_2}^{-1}$, (135) can be expressed as

$$\mathbf{M} = \mathbf{Q_2}^{-1\,\mathrm{T}}[\mathbf{P_2}^{\mathrm{T}}(\mathbf{Q_1} + \mathbf{Q_2M}^\alpha) - \mathbf{1}][\mathbf{Q_1} + \mathbf{Q_2M}^\alpha]^{-1} \quad . \tag{136}$$

We apply the symplectic property of paraxial ray propagator matrix (113), $\mathbf{P_2}^{\mathrm{T}}\mathbf{Q_1} - \mathbf{Q_2}^{\mathrm{T}}\mathbf{P_1} = \mathbf{1}$ and $\mathbf{P_2}^{\mathrm{T}}\mathbf{Q_2} - \mathbf{Q_2}^{\mathrm{T}}\mathbf{P_2} = \mathbf{0}$,

$$\mathbf{M} = \mathbf{Q_2}^{-1\,\mathrm{T}}\mathbf{Q_2}^{\mathrm{T}}[\mathbf{P_1} + \mathbf{P_2M}^\alpha][\mathbf{Q_1} + \mathbf{Q_2M}^\alpha]^{-1} \quad , \tag{137}$$

and arrive at

$$\mathbf{M} = [\mathbf{P_1} + \mathbf{P_2M}^\alpha][\mathbf{Q_1} + \mathbf{Q_2M}^\alpha]^{-1} \quad , \tag{138}$$

which describes the Gaussian beam given by initial conditions

$$\mathbf{M} = \mathbf{M}^\alpha \tag{139}$$

at point $\mathbf{x}^\alpha$ (Klimeš, 2004, eq. 50; Červený, Klimeš & Pšenčík, 2007, eq. 135). Defining the matrix

$$\boxed{\mathbf{Q} = \mathbf{Q}_1 + \mathbf{Q}_2\mathbf{M}^\alpha} \tag{140}$$

of geometrical spreading of the Gaussian beam, and matrix

$$\boxed{\mathbf{P} = \mathbf{P}_1 + \mathbf{P}_2\mathbf{M}^\alpha \quad ,} \tag{141}$$

equation (138) may be expressed in the form

$$\boxed{\mathbf{M} = \mathbf{PQ}^{-1} \quad .} \tag{142}$$

The paraxial expansion (95) of the complex–valued travel–time of the time–harmonic Gaussian beam scattered by Gabor function $g^\alpha(\mathbf{x})$ at frequency ω^0 in the local Cartesian coordinates reads

$$\boxed{T^\alpha_{\omega^0}(\mathbf{x}) = T^\alpha + \tau^0 + \tfrac{\mathrm{d}\tau}{\mathrm{d}q_3}\Delta x^{(q)}_3 + \tfrac{1}{2}\Delta x^{(q)}_i M_{ij}\Delta x^{(q)}_j \quad . \qquad (143)}$$

Matrix M_{ij} is given by (112) and (142). Note that (143) can be expressed in ray–centred coordinates as

$$T^\alpha_{\omega^0}(\mathbf{x}) = T^\alpha + \tau^\alpha(\mathbf{x}^\mathrm{R}(q_3)) + \tfrac{1}{2}\mathbf{q}^\mathrm{T}\mathbf{M}\mathbf{q} \quad . \qquad (144)$$

4.4.2. Complex–valued travel time of the Gaussian beam at frequency ω

We multiply matrix (129) by vector (131). The first two ray–centred components of vector $(\omega^0)^{-1}(\theta^{0\prime\prime}+\mathrm{i}\omega^{-1}K^\alpha)^{-1}_{ij}k^\alpha_j$ appearing in equation (96) then are

$$-[\mathbf{Q_2}^{-1}\mathbf{Q_1}+\mathbf{M}^\alpha]^{-1}\mathbf{M}^\alpha_4 \quad , \qquad (145)$$

where

$$\boxed{\mathbf{M}^\alpha_4 = -(\omega^0)^{-1}\left(\mathbf{k}^{(q)} - \frac{\mathbf{m}k^{(q)}_3}{m}\right) \quad . \qquad (146)}$$

The third ray–centred component of vector $(\omega^0)^{-1}(\theta^{0\prime\prime}+\mathrm{i}\omega^{-1}K^\alpha)^{-1}_{ij}k^\alpha_j$ is

$$\frac{(\omega^0)^{-1}k^{(q)}_3 + \mathbf{m}^\mathrm{T}[\mathbf{Q_2}^{-1}\mathbf{Q_1}+\mathbf{M}^\alpha]^{-1}\mathbf{M}^\alpha_4}{m} \quad . \qquad (147)$$

The first two ray–centred components of vector $(\omega^0)^{-1}\tau^{0\prime}_{,ij}(\theta^{0\prime\prime}+\mathrm{i}\omega^{-1}K^\alpha)^{-1}_{jk}k^\alpha_k$ appearing in equation (96) can be obtained from (120) and (145). They read

$$\mathbf{M}_4 = \mathbf{Q_2}^{-1\mathrm{T}}[\mathbf{Q_2}^{-1}\mathbf{Q_1}+\mathbf{M}^\alpha]^{-1}\mathbf{M}^\alpha_4 \quad , \qquad (148)$$

i.e.,

$$\mathbf{M}_4 = [\mathbf{Q_1}+\mathbf{Q_2}\mathbf{M}^\alpha]^{-1\mathrm{T}}\mathbf{M}^\alpha_4 \quad . \qquad (149)$$

The third component is zero. It is interesting that equation (149) for the space–frequency dependence of the scattered Gaussian beam has the same form as the equation for the space–time dependence of a Gaussian packet (Klimeš, 2004, eq. 74; Červený, Klimeš & Pšenčík, 2007, eq. 166). Considering definition (140), equation (149) may be expressed in the form

$$\boxed{\mathbf{M}_4 = \mathbf{Q}^{-1\mathrm{T}}\mathbf{M}^\alpha_4 \quad , \qquad (150)}$$

with initial conditions $\mathbf{M}_4 = \mathbf{M}^\alpha_4$.

Quantity

$$M_{44} = -(\omega^0)^{-2}k^\alpha_i(\theta^{0\prime\prime}+\mathrm{i}\omega^{-1}K^\alpha)^{-1}_{ij}k^\alpha_j \quad , \qquad (151)$$

appearing in equation (96) can be obtained from equations (131), (145), (146) and (147). It reads

$$\boxed{M_{44} = M^\alpha_{44} - \mathbf{M}^{\alpha\mathrm{T}}_4[\mathbf{Q_2}^{-1}\mathbf{Q_1}+\mathbf{M}^\alpha]^{-1}\mathbf{M}^\alpha_4 \quad , \qquad (152)}$$

where

$$\boxed{M^{\alpha}_{44} = -(\omega^0)^{-2}\,\frac{(k^{(q)}_3)^2}{m} \qquad . \qquad (153)}$$

It is interesting that equation (152) for the frequency dependence of the scattered Gaussian beam has the same form as the equation for the time dependence of a Gaussian packet (Klimeš, 2004, eq. 80; Červený, Klimeš & Pšenčík, 2007, eq. 167). Considering definition (140), equation (152) may be expressed in the form

$$M_{44} = M^{\alpha}_{44} - \mathbf{M}^{\alpha\,\mathrm{T}}_4\mathbf{Q}^{-1}\mathbf{Q_2}\mathbf{M}^{\alpha}_4 \qquad . \qquad (154)$$

The approximate frequency dependence (96) of the scattered Gaussian beam can be expressed in local Cartesian coordinates as

$$\boxed{T^{\alpha}_{\omega}(\mathbf{x}) = T^{\alpha}_{\omega^0}(\mathbf{x}) + \Delta x^{(q)}_K M_{K4}\,\tfrac{\Delta\omega}{\omega} + \tfrac{1}{2}M_{44}\left(\tfrac{\Delta\omega}{\omega}\right)^2 \qquad , \qquad (155)}$$

or in ray–centred coordinates as

$$T^{\alpha}_{\omega}(\mathbf{x}) = T^{\alpha}_{\omega^0}(\mathbf{x}) + \mathbf{q}^{\mathrm{T}}\mathbf{M}_4\,\tfrac{\Delta\omega}{\omega} + \tfrac{1}{2}M_{44}\left(\tfrac{\Delta\omega}{\omega}\right)^2 \qquad . \qquad (156)$$

4.4.3. Amplitude of the Gaussian beam

We express the complex–valued relative geometrical spreading in terms of the 2×2 submatrix $\mathbf{Q}_2(\mathbf{x},\mathbf{x}')$ of paraxial–ray propagator matrix (113) in ray–centred coordinates,

$$L(\mathbf{x},\mathbf{x}^{\alpha}) = \sqrt{\frac{h(\mathbf{x})\;h(\mathbf{x}^{\alpha})}{v(\mathbf{x})\frac{\mathrm{d}\tau}{\mathrm{d}q_3}(\mathbf{x})\;v(\mathbf{x}^{\alpha})\frac{\mathrm{d}\tau}{\mathrm{d}q_3}(\mathbf{x}^{\alpha})}\;\det[\mathbf{Q}_2(\mathbf{x},\mathbf{x}^{\alpha})]} \qquad . \qquad (157)$$

Jacobian h is defined by (103), and v is the phase velocity, see (21). Relative geometrical spreading (157) should correctly include possible phase shifts due to caustics.

We insert expression (157) into equation (79). Then the product of the determinants in (79) can be expressed using (126) as

$$\det(\mathbf{Q}_2)\;\det(K^{\alpha}_{ij} - \mathrm{i}\omega\theta^{0\prime\prime}_{,kl}) = [h(\mathbf{x}^{\alpha})]^{-2}\det\!\left[-\mathrm{i}\omega\begin{pmatrix}\mathbf{Q_1}+\mathbf{Q_2}(\mathbf{T}^{(q)}+\mathrm{i}\omega^{-1}\mathbf{K}^{(q)}) & \mathbf{Q_2 m}\\ \mathbf{m}^{\mathrm{T}} & m\end{pmatrix}\right] . \qquad (158)$$

We may multiply the third column of the matrix at the right–hand side of (158) by $\frac{\mathbf{m}^{\mathrm{T}}}{m}$ and subtract the product from the first two columns,

$$\begin{aligned}&\det(\mathbf{Q}_2)\;\det(K^{\alpha}_{ij} - \mathrm{i}\omega\theta^{0\prime\prime}_{,kl})\\ &\quad = [h(\mathbf{x}^{\alpha})]^{-2}\det\!\left[-\mathrm{i}\omega\begin{pmatrix}\mathbf{Q_1}+\mathbf{Q_2}(\mathbf{T}^{(q)}+\mathrm{i}\omega^{-1}\mathbf{K}^{(q)}-\frac{\mathbf{m}\,\mathbf{m}^{\mathrm{T}}}{m}) & \mathbf{Q_2 m}\\ \mathbf{0}^{\mathrm{T}} & m\end{pmatrix}\right] . \qquad (159)\end{aligned}$$

Considering (130) and (140),

$$\det(\mathbf{Q}_2)\;\det(K^{\alpha}_{ij} - \mathrm{i}\omega\theta^{0\prime\prime}_{,kl}) = [h(\mathbf{x}^{\alpha})]^{-2}\det\!\left[-\mathrm{i}\omega\begin{pmatrix}\mathbf{Q} & \mathbf{Q_2 m}\\ \mathbf{0}^{\mathrm{T}} & m\end{pmatrix}\right] \qquad , \qquad (160)$$

i.e.,

$$\det(\mathbf{Q}_2)\;\det(K^{\alpha}_{ij} - \mathrm{i}\omega\theta^{0\prime\prime}_{,kl}) = [h(\mathbf{x}^{\alpha})]^{-2}(-\mathrm{i}\omega m)\;\det(-\mathrm{i}\omega\mathbf{Q}) \qquad . \qquad (161)$$

We insert (161) into (79) with (157),

$$\widehat{a}(\mathbf{x},\omega) = R(\mathbf{x},\mathbf{x}^\alpha)\sqrt{\frac{\varrho(\mathbf{x}^\alpha)\frac{\mathrm{d}\tau}{\mathrm{d}q_3}(\mathbf{x})\frac{\mathrm{d}\tau}{\mathrm{d}q_3}(\mathbf{x}^\alpha)h(\mathbf{x}^\alpha)}{\varrho(\mathbf{x})h(\mathbf{x})}}\,\frac{\omega\widehat{A}(\mathbf{x}^\alpha,\omega)\,r^\alpha(\mathbf{x})}{\sqrt{\det[-\mathrm{i}\mathbf{Q}(\mathbf{x},\mathbf{x}^\alpha)]}}\,\frac{\sqrt{2\pi}}{\sqrt{-\mathrm{i}\omega m}} \quad . \tag{162}$$

The initial value of the amplitude of the Gaussian beam at point $\mathbf{x}^\alpha$ reads

$$\boxed{\widehat{a}(\mathbf{x}^\alpha,\omega) = \mathrm{i}\omega\widehat{A}(\mathbf{x}^\alpha,\omega)\; r^\alpha(\mathbf{x})\; \tfrac{\mathrm{d}\tau}{\mathrm{d}q_3}(\mathbf{x}^\alpha)\frac{\sqrt{2\pi}}{\sqrt{-\mathrm{i}\omega m}} \quad .} \tag{163}$$

When determining the sign of $\sqrt{\det[-\mathrm{i}\mathbf{Q}(\mathbf{x},\mathbf{x}^\alpha)]}$ at point $\mathbf{x}=\mathbf{x}^\alpha$, we took into account that matrix $\mathbf{Q}(\mathbf{x},\mathbf{x}^\alpha)$ is unit at $\mathbf{x}=\mathbf{x}^\alpha$, but has a small positive–definite imaginary part along the ray in the vicinity of $\mathbf{x}^\alpha$.

We now express the amplitude of the Gaussian beam in terms of its initial value (163),

$$\boxed{\widehat{a}(\mathbf{x},\omega) = R(\mathbf{x},\mathbf{x}^\alpha)\sqrt{\frac{\varrho(\mathbf{x}^\alpha)\frac{\mathrm{d}\tau}{\mathrm{d}q_3}(\mathbf{x})h(\mathbf{x}^\alpha)}{\varrho(\mathbf{x})\frac{\mathrm{d}\tau}{\mathrm{d}q_3}(\mathbf{x}^\alpha)h(\mathbf{x})}}\,\frac{1}{\sqrt{\det[\mathbf{Q}(\mathbf{x},\mathbf{x}^\alpha)]}}\,\widehat{a}(\mathbf{x}^\alpha,\omega) \quad .} \tag{164}$$

Here $v(\mathbf{x})$ is the phase velocity, $\varrho(\mathbf{x})$ is the density, $\mathbf{Q}(\mathbf{x},\mathbf{x}^\alpha)$ is the complex–valued matrix of geometrical spreading of the Gaussian beam, and $R(\mathbf{x},\mathbf{x}')$ is the accumulated reciprocal transmission coefficient describing amplitude losses between points $\mathbf{x}'$ and $\mathbf{x}$ due to attenuation and due to reflections and scattering into directions leading outside the vicinity of point $\mathbf{x}$. Reflectivity function r^α in (163) is given by (68) and m is defined by (128). Term $\sqrt{\det[\mathbf{Q}(\mathbf{x},\mathbf{x}^\alpha)]}$ is equal to 1 at $\mathbf{x}=\mathbf{x}^\alpha$, and then varies continuously along the ray.

4.4.4. Note on "effective relative slowness perturbation"

We define the "effective second derivatives of travel time" by equation

$$T^{\mathrm{eff}}_{,ij} = T^\alpha_{,ij} - T^{\mathrm{ray}}_{,ij} \quad . \tag{165}$$

The second derivatives $T^\alpha_{,ij}$ of travel time of the incident wave are defined by equation (38). They include both the second derivatives of travel time due to the curvature of the wavefront and due to the curvature of the ray. Matrix

$$T^{\mathrm{ray}}_{,ij} = -H_{,i}p_j - p_iH_{,j} + p_ip_jH^{,m}H_{,m} \tag{166}$$

corresponds to the scattered wave and contains only the second derivatives (109) of travel time due to the curvature of the ray. Derivatives $H^{,i}$ and $H_{,i}$ of the homogeneous Hamiltonian, defined by (102), correspond to the central ray of the Gaussian beam scattered at point $\mathbf{x}^\alpha$. In ray–centred coordinates, matrix $T^\alpha_{,ij}$ is given by equation (122), and matrix $T^{\mathrm{ray}}_{,ij}$ can be described by equation (133) with $\mathbf{M}=\mathbf{0}$, $\mathbf{M}_3=\mathbf{M}^\alpha_3$ and $M_{33}=M^\alpha_{33}$.

Matrix $T^{\mathrm{eff}}_{,ij}+\mathrm{i}\omega^{-1}K^\alpha_{ij}$ can be expressed in ray–centred coordinates in terms of quantities (127), (128) and (130) as

$$\begin{pmatrix} \mathbf{M}^\alpha + \frac{\mathbf{m}\mathbf{m}^{\mathrm{T}}}{m} & \mathbf{m} \\ \mathbf{m}^{\mathrm{T}} & m \end{pmatrix} \quad , \tag{167}$$

where m is related to the effective second derivatives (165) of travel time through equation

$$m = H^{,i}(T^{\rm eff}_{,ij} + {\rm i}\omega^{-1}K^\alpha_{ij})H^{,j}\,(\tfrac{{\rm d}\tau}{{\rm d}q_3})^2 \quad , \tag{168}$$

see (99). Then

$$(T^{\rm eff}_{,ij} + {\rm i}\omega^{-1}K^\alpha_{ij})(x_i - x^\alpha_i)(x_j - x^\alpha_j) = \mathbf{q}^{\rm T}\mathbf{M}^\alpha\mathbf{q} + m\,(q_3 - q^\alpha_3 + \tfrac{\mathbf{m}^{\rm T}}{m}\mathbf{q})^2 \quad , \tag{169}$$

where $x^{\rm R}_i(q^\alpha_3) = x^\alpha_i$. We may consider plane wave with amplitude $\widehat{A}(\mathbf{x}^\alpha,\omega)$ incident in direction p^0_i onto relative slowness perturbation

$$-\tfrac{\delta v}{v}(\mathbf{x}) = r^\alpha(\mathbf{x})\,\exp[\tfrac{1}{2}(x_i - x^\alpha_i)(-K^\alpha_{ij} + {\rm i}\omega T^{\rm eff}_{,ij})(x_j - x^\alpha_j)] \quad . \tag{170}$$

The corresponding travel–time perturbation

$$\delta\tau = \int\!{\rm d}\tau\,(-\tfrac{\delta v}{v}) = \int\!{\rm d}q_3\,\frac{{\rm d}\tau}{{\rm d}q_3}\,(-\tfrac{\delta v}{v}) \tag{171}$$

calculated in ray–centred coordinates then reads

$$\delta\tau(\mathbf{q}) = r^\alpha(\mathbf{q})\,\frac{{\rm d}\tau}{{\rm d}q_3}\frac{\sqrt{2\pi}}{\sqrt{-{\rm i}\omega m}}\exp({\rm i}\omega\tfrac{1}{2}\mathbf{q}^{\rm T}\mathbf{M}^\alpha\mathbf{q}) \quad . \tag{172}$$

The corresponding first–order perturbation of the incident plane wave is then equal to the scattered Gaussian beam with initial amplitude (163). Factor $\frac{{\rm d}\tau}{{\rm d}q_3}\sqrt{2\pi}/\sqrt{-{\rm i}\omega m}$ in (163) thus represents the integral of function

$$\exp[-\tfrac{1}{2}(x_i - x^\alpha_i)(K^\alpha_{ij} - {\rm i}\omega T^{\rm eff}_{,ij})(x_j - x^\alpha_j)] \tag{173}$$

with respect to travel time along the central ray of the scattered Gaussian beam.

Inverse matrix $(T^{\rm eff} + {\rm i}\omega^{-1}K^\alpha)^{-1}_{,ij}$ in ray–centred coordinates reads

$$\begin{pmatrix} \mathbf{M}^{\alpha\,-1} & -\mathbf{M}^{\alpha\,-1}\frac{\mathbf{m}}{m} \\ -\frac{\mathbf{m}^{\rm T}}{m}\mathbf{M}^{\alpha\,-1} & \frac{1}{m} + \frac{\mathbf{m}^{\rm T}\mathbf{M}^{\alpha\,-1}\mathbf{m}}{m^2} \end{pmatrix} \quad . \tag{174}$$

We thus see that inverse matrix $\mathbf{M}^{\alpha\,-1}$ to matrix $\mathbf{M}^\alpha$, which describes the initial shape of the Gaussian beam, represents the projection of matrix $(T^{\rm eff} + {\rm i}\omega^{-1}K^\alpha)^{-1}_{,ij}$ inverse to matrix $T^{\rm eff}_{,ij} + {\rm i}\omega^{-1}K^\alpha_{ij}$ onto the wavefront tangent plane,

$$M^{\alpha\,-1}_{\;KL} = \widehat{h}^K_i\,(T^{\rm eff} + {\rm i}\omega^{-1}K^\alpha)^{-1}_{,ij}\,\widehat{h}^L_j \quad . \tag{175}$$

This projection onto the wavefront tangent plane is performed in the direction of the ray.

4.5. Central rays of the Gaussian beams

The central ray of the Gaussian beam scattered at frequency ω^0 is determined by initial point $\mathbf{x}^\alpha$ and initial slowness vector p_i^0. The central ray of the Gaussian beam scattered at slightly different frequency ω is close to this ray, but is different. It does not pass exactly through point $\mathbf{x}^\alpha$ and its initial slowness vector is slightly different from p_i^0.

4.5.1. Frequency dependence of the central rays of the Gaussian beams

At frequency ω^0 given by equations (90) and (91), the central ray of the Gaussian beam is determined by initial point $\mathbf{x}^\alpha$ and initial slowness vector p_i^0, see equation (143) or (144). At frequencies ω from the vicinity of ω^0, the central ray of the Gaussian beam is deviated. In the ray–centred coordinates q_i, attached to the axial ray with initial point $\mathbf{x}^\alpha$ and initial slowness vector p_i^0, the central ray of the Gaussian beam is

$$\overline{\mathbf{q}} = -(\mathrm{Im}\mathbf{M})^{-1}\mathrm{Im}\mathbf{M}_4\tfrac{\Delta\omega}{\omega} \quad . \tag{176}$$

see equations (143) and (155). Inserting equation (150) and identity (Klimeš, 2004, eq. 75)

$$\mathrm{Im}\mathbf{M} = {\mathbf{Q}^{-1}}^{\mathrm{T}}\mathrm{Im}\mathbf{M}^\alpha{\mathbf{Q}^{-1}}^{*} \tag{177}$$

into equation (176), we arrive at

$$\overline{\mathbf{q}} = -\mathrm{Im}[\mathbf{Q}^*(\mathrm{Im}\mathbf{M}^\alpha)^{-1}\mathbf{M}_4^\alpha]\tfrac{\Delta\omega}{\omega} \quad . \tag{178}$$

Considering definition (140), equation (178) may be expressed as

$$\overline{\mathbf{q}}=\{-\mathbf{Q}_1(\mathrm{Im}\mathbf{M}^\alpha)^{-1}\mathrm{Im}\mathbf{M}_4^\alpha+\mathbf{Q}_2[\mathrm{Im}\mathbf{M}^\alpha(\mathrm{Im}\mathbf{M}^\alpha)^{-1}\mathrm{Re}\mathbf{M}_4^\alpha-\mathrm{Re}\mathbf{M}^\alpha(\mathrm{Im}\mathbf{M}^\alpha)^{-1}\mathrm{Im}\mathbf{M}_4^\alpha]\}\tfrac{\Delta\omega}{\omega} \, . \tag{179}$$

Equation (179) describes the paraxial ray

$$\overline{\mathbf{q}} = \mathbf{Q}_1\overline{\mathbf{q}}^\alpha + \mathbf{Q}_2\overline{\mathbf{p}}^{(q)\alpha} \tag{180}$$

with initial conditions

$$\overline{\mathbf{q}}^\alpha = -(\mathrm{Im}\mathbf{M}^\alpha)^{-1}\mathrm{Im}\mathbf{M}_4^\alpha\tfrac{\Delta\omega}{\omega} \tag{181}$$

and

$$\overline{\mathbf{p}}^{(q)\alpha} = [\mathrm{Re}\mathbf{M}_4^\alpha - \mathrm{Re}\mathbf{M}^\alpha(\mathrm{Im}\mathbf{M}^\alpha)^{-1}\mathrm{Im}\mathbf{M}_4^\alpha]\tfrac{\Delta\omega}{\omega} = \mathrm{Re}\mathbf{M}_4^\alpha\tfrac{\Delta\omega}{\omega} + \mathrm{Re}\mathbf{M}^\alpha\overline{\mathbf{q}}^\alpha \quad . \tag{182}$$

Equation (180) determines the central ray of the Gaussian beam scattered at frequency ω in the ray centred coordinates corresponding to frequency ω^0. The paraxial approximation of the slowness–vector corresponding to paraxial ray (180) is

$$\overline{\mathbf{p}}^{(q)} = \mathbf{P}_1\overline{\mathbf{q}}^\alpha + \mathbf{P}_2\overline{\mathbf{p}}^{(q)\alpha} \quad . \tag{183}$$

The central ray of the Gaussian beam is given by initial position (181) and initial slowness vector (182).

4.5.2. Shape of the Gaussian beams

We denote by $\widetilde{\mathbf{q}}$ the ray–centered coordinates measured from the frequency–dependent central ray (180) of the Gaussian beam,

$$\mathbf{q} = \overline{\mathbf{q}} + \widetilde{\mathbf{q}} \quad . \tag{184}$$

Note that the coordinate planes of $\widetilde{\mathbf{q}}$ are still tangent to wavefronts along ray $\mathbf{q} = \mathbf{0}$, not along ray $\widetilde{\mathbf{q}} = \mathbf{0}$.

Paraxial expansion (156) with (144) of the complex–valued travel–time of the Gaussian beam in ray–centered coordinates $\mathbf{q}$ reads

$$T^\alpha_\omega(\mathbf{x}) = T^\alpha + \tau^\alpha(\mathbf{x}^{\mathrm{R}}(q_3)) + \tfrac{1}{2}\mathbf{q}^{\mathrm{T}}\mathbf{M}\mathbf{q} + \mathbf{q}^{\mathrm{T}}\mathbf{M}_4\tfrac{\Delta\omega}{\omega} + \tfrac{1}{2}M_{44}(\tfrac{\Delta\omega}{\omega})^2 \quad . \tag{185}$$

In coordinates $\widetilde{\mathbf{q}}$ measured from the central ray of the scattered Gaussian beam, we shall analogously write

$$T^\alpha_\omega(\mathbf{x}) = T^\alpha + \widetilde{\tau}^\alpha(\widetilde{\mathbf{x}}^{\mathrm{R}}(q_3)) + \tfrac{1}{2}\widetilde{\mathbf{q}}^{\mathrm{T}}\mathbf{M}\widetilde{\mathbf{q}} + \widetilde{\mathbf{q}}^{\mathrm{T}}\widetilde{\mathbf{M}}_4\tfrac{\Delta\omega}{\omega} + \tfrac{1}{2}\widetilde{M}_{44}(\tfrac{\Delta\omega}{\omega})^2 \quad , \tag{186}$$

where

$$\widetilde{\tau}^\alpha(\widetilde{\mathbf{x}}^{\mathrm{R}}(q_3)) = \tau^\alpha(\mathbf{x}^{\mathrm{R}}(q_3)) + \tfrac{1}{2}\overline{\mathbf{p}}^{(q)^{\mathrm{T}}}\overline{\mathbf{q}} + \overline{\mathbf{p}}^{(q)^{\mathrm{T}}}\widetilde{\mathbf{q}} \tag{187}$$

is the linear Taylor expansion of travel time in coordinates $\widetilde{\mathbf{q}}$. Inserting (184) into (185) and comparing the result with equations (186) and (187), we obtain

$$\widetilde{\mathbf{M}}_4 = \mathbf{M}_4 + \mathbf{M}\overline{\mathbf{q}}\tfrac{\omega}{\Delta\omega} - \overline{\mathbf{p}}^{(q)}\tfrac{\omega}{\Delta\omega} \tag{188}$$

and

$$\widetilde{M}_{44} = M_{44} + 2\mathbf{M}_4{}^{\mathrm{T}}\overline{\mathbf{q}}\tfrac{\omega}{\Delta\omega} + \overline{\mathbf{q}}^{\mathrm{T}}\mathbf{M}\overline{\mathbf{q}}(\tfrac{\omega}{\Delta\omega})^2 - \overline{\mathbf{p}}^{(q)^{\mathrm{T}}}\overline{\mathbf{q}}(\tfrac{\omega}{\Delta\omega})^2 \quad . \tag{189}$$

Considering (188), equation (189) reads

$$\widetilde{M}_{44} = M_{44} + \mathbf{M}_4{}^{\mathrm{T}}\overline{\mathbf{q}}\tfrac{\omega}{\Delta\omega} + \widetilde{\mathbf{M}}_4^{\mathrm{T}}\overline{\mathbf{q}}\tfrac{\omega}{\Delta\omega} \quad . \tag{190}$$

Inserting (138), (140), (150), and (180) into (188), we obtain

$$\widetilde{\mathbf{M}}_4 = \mathbf{Q}^{-1^{\mathrm{T}}}[\mathbf{M}^\alpha_4 + (\mathbf{P_1}{}^{\mathrm{T}} + \mathbf{M}^\alpha\mathbf{P_2}{}^{\mathrm{T}})(\mathbf{Q_1}\overline{\mathbf{q}}^\alpha + \mathbf{Q_2}\overline{\mathbf{p}}^{(q)\alpha})\tfrac{\omega}{\Delta\omega}] - \overline{\mathbf{p}}^{(q)^{\mathrm{T}}}\tfrac{\omega}{\Delta\omega} \quad . \tag{191}$$

Using the symplectic property of the paraxial ray propagator matrix, equation (191) may be expressed as

$$\widetilde{\mathbf{M}}_4 = \mathbf{Q}^{-1^{\mathrm{T}}}\{\mathbf{M}^\alpha_4 + [(\mathbf{Q_1}{}^{\mathrm{T}} + \mathbf{M}^\alpha\mathbf{Q_2}{}^{\mathrm{T}})(\mathbf{P_1}\overline{\mathbf{q}}^\alpha + \mathbf{P_2}\overline{\mathbf{p}}^{(q)\alpha}) + \mathbf{M}^\alpha\overline{\mathbf{q}}^\alpha - \overline{\mathbf{p}}^{(q)\alpha}]\tfrac{\omega}{\Delta\omega}\} - \overline{\mathbf{p}}^{(q)^{\mathrm{T}}}\tfrac{\omega}{\Delta\omega} \, . \tag{192}$$

Inserting (181) and (182) into (192), $\mathbf{M}^\alpha_4$ cancels with $(\mathbf{M}^\alpha\overline{\mathbf{q}}^\alpha - \overline{\mathbf{p}}^{(q)\alpha})\frac{\omega}{\Delta\omega}$ and we obtain

$$\widetilde{\mathbf{M}}_4 = \mathbf{0} \quad . \tag{193}$$

Considering (149), equation (152) can be expressed as

$$M_{44} = -\mathbf{M}_4{}^{\mathrm{T}}\mathbf{Q_2}\mathbf{M}^\alpha_4 + M^\alpha_{44} \quad . \tag{194}$$

Equation (190) with (194) and (193) reads

$$\widetilde{M}_{44} = \mathbf{M}_4{}^{\mathrm{T}}[\overline{\mathbf{q}}\tfrac{\omega}{\Delta\omega} - \mathbf{Q_2}\mathbf{M}^\alpha_4] + M^\alpha_{44} \quad . \tag{195}$$

Inserting (180) with (181) and (182),

$$\widetilde{M}_{44} = -\mathbf{M}_4{}^{\mathrm{T}}[\mathbf{Q_1} + \mathbf{Q_2}\mathbf{M}^\alpha](\mathrm{Im}\mathbf{M}^\alpha)^{-1}\mathrm{Im}\mathbf{M}^\alpha_4 + M^\alpha_{44} \quad . \tag{196}$$

Inserting (150), we arrive at

$$\widetilde{M}_{44} = -\mathbf{M}_4^{\alpha\,\mathrm{T}} (\mathrm{Im}\mathbf{M}^\alpha)^{-1} \mathrm{Im}\mathbf{M}_4^\alpha + M_{44}^\alpha \quad , \tag{197}$$

and see that $\widetilde{M}_{44}$ is constant along the central ray of the Gaussian beam as we expected. Considering (181), we see that

$$\widetilde{M}_{44} (\tfrac{\Delta\omega}{\omega})^2 = \mathbf{M}_4^{\alpha\,\mathrm{T}} \overline{\mathbf{q}}^\alpha \tfrac{\Delta\omega}{\omega} + M_{44}^\alpha (\tfrac{\Delta\omega}{\omega})^2 \quad . \tag{198}$$

Note that equation (198) is also a direct consequence of equation (156) and of the definition of $\overline{\mathbf{q}}$.

4.5.3. Frequency dependence of the amplitude of the Gaussian beams

Frequency dependence of the amplitude of the Gaussian beams is given by multiplication factor

$$\exp[\mathrm{i}\omega \tfrac{1}{2} \widetilde{M}_{44} (\tfrac{\Delta\omega}{\omega})^2] \quad , \tag{199}$$

see equation (186) with (193).

For given frequency ω, we may also consider the dependence of the multiplication factor (199) on structural wavenumbers. In the wavenumber domain, the point of intersection of the wavenumber surface (81) with the half–line leading from the origin in the direction of k_i^α is $\frac{\omega^0}{\omega} k_i^\alpha$. The vectorial difference between k_i^α and the point of intersection is

$$\Delta k_i^\alpha = \tfrac{\Delta\omega}{\omega} k_i^\alpha \quad . \tag{200}$$

In ray–centred coordinates,

$$\Delta k_i^{(q)} = \tfrac{\Delta\omega}{\omega} k_i^{(q)} \quad . \tag{201}$$

The unit vector perpendicular to the wavenumber surface (81) is

$$n_i = h_3^i \tfrac{\mathrm{d}q_3}{\mathrm{d}s} \quad , \tag{202}$$

where s is the arclength along the ray. Then the perpendicular distance between k_i^α and the wavenumber surface (81) is

$$\Delta k = n_i \, \Delta k_i^\alpha = \tfrac{\mathrm{d}q_3}{\mathrm{d}s} \tfrac{\Delta\omega}{\omega} k_3^{(q)} = \tfrac{\mathrm{d}q_3}{\mathrm{d}s} \Delta k_3^{(q)} \quad . \tag{203}$$

Inserting (146) and (153) into (197), we obtain

$$\widetilde{M}_{44} = (\omega^0)^{-1} (\mathrm{Im}\tfrac{\mathbf{m}}{m})^{\mathrm{T}} (\omega^0 \mathrm{Im}\mathbf{M}^\alpha)^{-1} (\mathbf{k}^{(q)} - \tfrac{\mathbf{m}}{m} k_3^{(q)}) \, k_3^{(q)} - (\omega^0)^{-2} \tfrac{1}{m} (k_3^{(q)})^2 \quad . \tag{204}$$

Considering (201), we may express multiplication factor (199) with (204) in form

$$\exp\{\tfrac{1}{2}\mathrm{i}\tfrac{\omega}{\omega^0}[(\mathrm{Im}\tfrac{\mathbf{m}}{m})^{\mathrm{T}} (\omega^0 \mathrm{Im}\mathbf{M}^\alpha)^{-1} (\Delta\mathbf{k}^{(q)} - \tfrac{\mathbf{m}}{m} \Delta k_3^{(q)}) \, \Delta k_3^{(q)} - \tfrac{1}{\omega^0 m} (\Delta k_3^{(q)})^2]\} \quad , \tag{205}$$

and after approximation $\frac{\omega}{\omega^0} \approx 1$ as

$$\exp\{\tfrac{1}{2}\mathrm{i}[(\mathrm{Im}\tfrac{\mathbf{m}}{m})^{\mathrm{T}} (\omega^0 \mathrm{Im}\mathbf{M}^\alpha)^{-1} (\Delta\mathbf{k}^{(q)} - \tfrac{\mathbf{m}}{m} \Delta k_3^{(q)}) \, \Delta k_3^{(q)} - \tfrac{1}{\omega^0 m} (\Delta k_3^{(q)})^2]\} \quad . \tag{206}$$

The absolute value of factor (206) depends on $\Delta k_3^{(q)}$ only,

$$\exp\{\tfrac{1}{2}[\mathrm{Im}\tfrac{1}{\omega^0 m} + (\mathrm{Im}\tfrac{\mathbf{m}}{m})^{\mathrm{T}} (\omega^0 \mathrm{Im}\mathbf{M}^\alpha)^{-1} \, \mathrm{Im}\tfrac{\mathbf{m}}{m}] \, (\Delta k_3^{(q)})^2\} \quad . \tag{207}$$

In terms of the perpendicular distance between k_i^α and the wavenumber surface,

$$\exp\{\tfrac{1}{2}[\mathrm{Im}\tfrac{1}{\omega^0 m} + (\mathrm{Im}\tfrac{\mathbf{m}}{m})^{\mathrm{T}} (\omega^0 \mathrm{Im}\mathbf{M}^\alpha)^{-1} \, \mathrm{Im}\tfrac{\mathbf{m}}{m}] \, (\tfrac{\mathrm{d}s}{\mathrm{d}q_3})^2 (\Delta k)^2\} \quad . \tag{208}$$

4.6. Review of scattered Gaussian beams

For each frequency ω, the scattered wavefield consists of at most one P–wave Gaussian beam or of at most two S–wave Gaussian beams. A Gaussian beam is generated if structural wavenumber vector k^{α} is close to the corresponding *"wavenumber surface"* $\mathcal{S}_{\mathbf{P}\omega}$, defined by transformation

$$\mathbf{p} \in \mathcal{S} \longrightarrow \mathbf{k} = (\mathbf{p} - \mathbf{P})\omega \in \mathcal{S}_{\mathbf{P}\omega} \tag{209}$$

of the slowness surface $\mathcal{S}$, see (81). For each frequency ω, the wavenumber surface is parametrized by initial slowness vectors $\mathbf{p}^0$ of generated Gaussian beams. The transformation for an incident P wave is illustrated in Figures 4, 5 and 6.

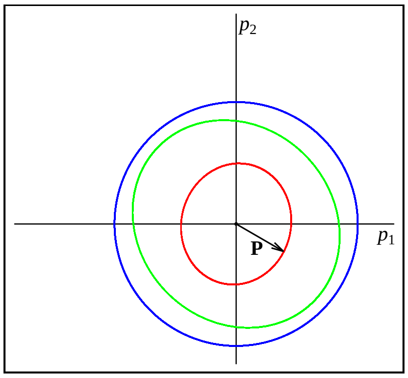

Figure 4. Slowness surface $\mathcal{S}$.

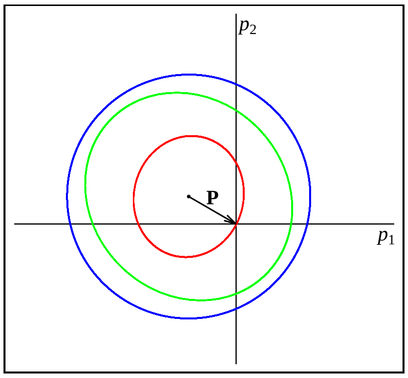

Figure 5. Shifted slowness surface $\mathcal{S}_{\mathbf{P}}$.

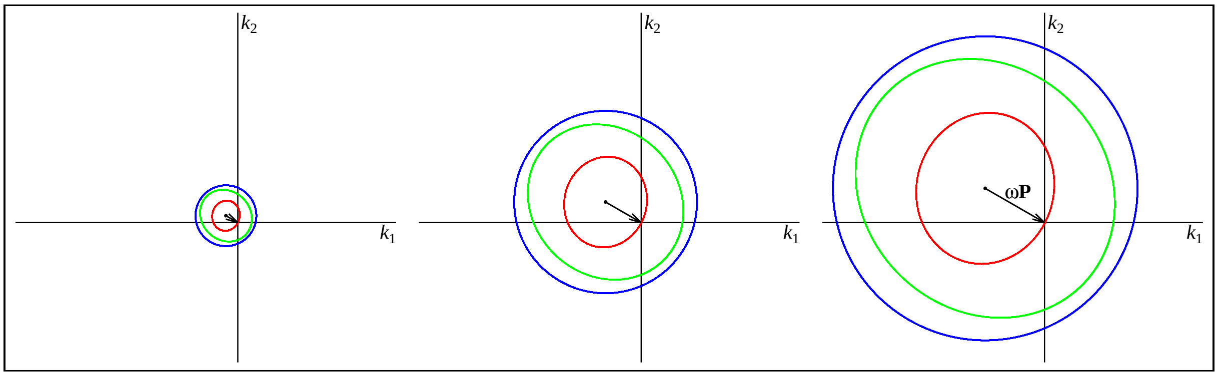

Figure 6. Wavenumber surfaces $\mathcal{S}_{\mathbf{P}\omega}$ at various positive frequencies ω.

The initial amplitude of the Gaussian beam scattered by Gabor function $g^{\alpha}(\mathbf{x})$ with $\mathbf{k}^{\alpha}$ situated at the wavenumber surface $\mathcal{S}_{\mathbf{P}\omega}$ corresponding to positive frequency ω is given by equation (163), in which reflectivity function r^{α} is given by (68) and m is defined by (128). For $\mathbf{k}^{\alpha} \in \mathcal{S}_{\mathbf{P}\omega}$, the central ray of the scattered Gaussian beam pass through point $\mathbf{x}^{\alpha}$, and its initial slowness vector is

$$\mathbf{p}^0 = \mathbf{P} + \omega^{-1}\mathbf{k}^{\alpha} \quad , \tag{210}$$

see (91). The initial shape of the Gaussian beam is determined in ray–centred coordinates by matrix $\mathbf{M}^{\alpha}$ defined by equation (130).

For $\mathbf{k}^{\alpha}$ from the vicinity of wavenumber surface $\mathcal{S}_{\mathbf{P}\omega}$, the initial point and initial slowness vector of the central ray of the scattered Gaussian beam slightly depend on $\mathbf{k}^{\alpha}$ through equations (146), (181) (182) and (201). For $\mathbf{k}^{\alpha}$ from the vicinity of wavenumber surface $\mathcal{S}_{\mathbf{P}\omega}$, the initial amplitude of the Gaussian beam exponentially decrease with the square of distance Δk from the wavenumber surface $\mathcal{S}_{\mathbf{P}\omega}$ according to equation (208). Gaussian weighting factor (208) of the initial amplitude of the Gaussian beam in the vicinity of wavenumber surface $\mathcal{S}_{\mathbf{P}\omega}$ is illustrated in Figures 7 and 8.

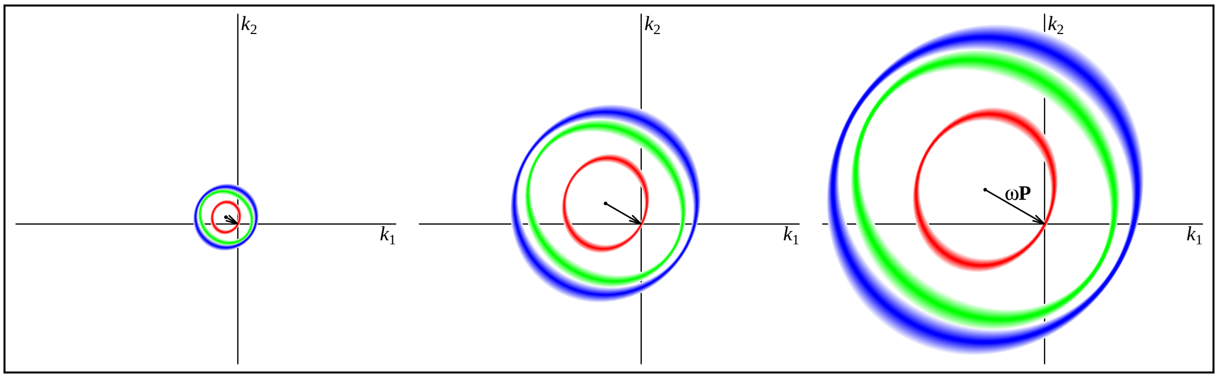

Figure 7. Sensitivity of scattered Gaussian beams to structural wavenumbers at various positive frequencies ω for an incident P wave. The sensitivity is given by Gaussian weighting factor (208).

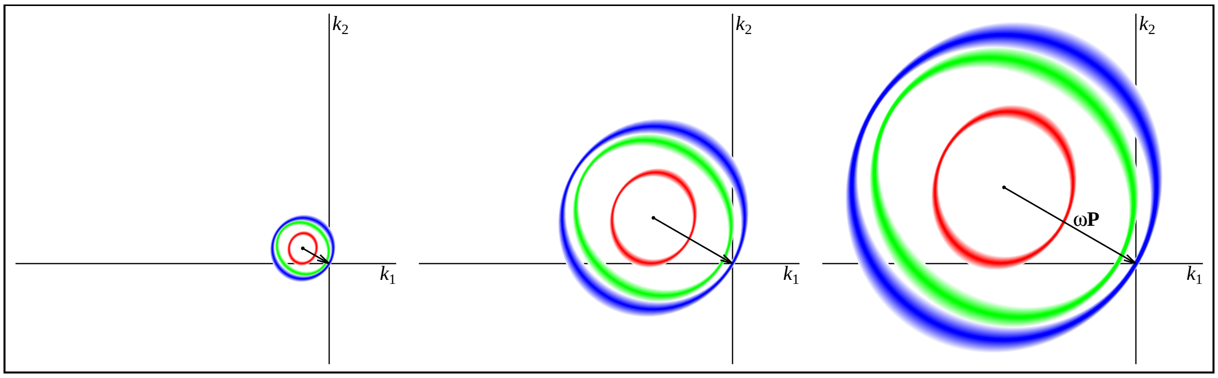

Figure 8. Sensitivity of scattered Gaussian beams to structural wavenumbers at various positive frequencies ω for an incident slower S wave. The sensitivity is given by Gaussian weighting factor (208).

A scattered Gaussian beam has a maximum amplitude if $\Delta k = 0$, i.e., if $\mathbf{k}^{\alpha} \in \mathcal{S}_{\mathbf{P}\omega}$. For each $\mathbf{k}^{\alpha}$, there are at most 5 finite positive frequencies $\omega = \omega_0$ such that $\mathbf{k}^{\alpha} \in \mathcal{S}_{\mathbf{P}\omega_0}$. The frequencies ω_0 are solutions of sixth–order equation (90). The equation has one infinite trivial solution $\omega_0 = +\infty$.

5. Scattering in the time domain — Gaussian packets

Scattered waves in the time domain are composed of the scattered frequency–domain Gaussian beams. The Gaussian frequency dependence (199) of the amplitude of the scattered Gaussian beam generates a Gaussian packet in the time domain.

For fixed $\mathbf{k}^\alpha$, the initial point and initial slowness vector of the central ray of the scattered Gaussian beam slightly depend on frequency through equations (181) and (182), scattering different frequencies to different directions. This phenomenon results in asymmetric Gaussian packets (Klimeš, 2004, fig. 1; Červený, Klimeš & Pšenčík, 2007, fig. 23).

5.1. Narrow–band scattering

There are at most 5 finite positive frequencies $\omega = \omega_0$ such that $\mathbf{k}^\alpha \in \mathcal{S}_{\mathbf{P}\omega_0}$. If $\mathbf{k}^\alpha$ is sufficiently deviated from the tangent plane to $\mathcal{S}_{\mathbf{P}\omega_0}$ at $\mathbf{k}^\alpha$, the beams are scattered in a narrow Gaussian frequency band centred at ω_0, forming a space–time Gaussian wave packet of prevailing frequency ω_0. Since vector $h_3^i(\mathbf{x}^\alpha)$, defined by (99) at point $\mathbf{x}^\alpha$, is perpendicular to wavenumber surface $\mathcal{S}_{\mathbf{P}\omega_0}$ at $\mathbf{k}^\alpha$, the mentioned deviation can be measured by $k_3^{(q)}$, see (203). A sufficient deviation of $\mathbf{k}^\alpha$ from the tangent plane to $\mathcal{S}_{\mathbf{P}\omega_0}$ at $\mathbf{k}^\alpha$ then means sufficiently large $k_3^{(q)}$ in equation (153).

We shall refer to the set of wavenumber vectors $\mathbf{k}^\alpha$, causing narrow–band scattering, as the "high–wavenumber domain", see Figures 9 and 10. For each particular broad–band incident wave, the wavefield, scattered by a Gabor function belonging to this domain, consists of at most 5 narrow–band space–time Gaussian wave packets. Each recorded Gaussian packet is localized in the time section (set of seismograms corresponding to the source).

This is typical wide–angle scattering, but occurs also for P to S or S to P forward and narrow–angle scattering. The high–wavenumber domain is usually being recovered by seismic migration or by diffraction tomography.

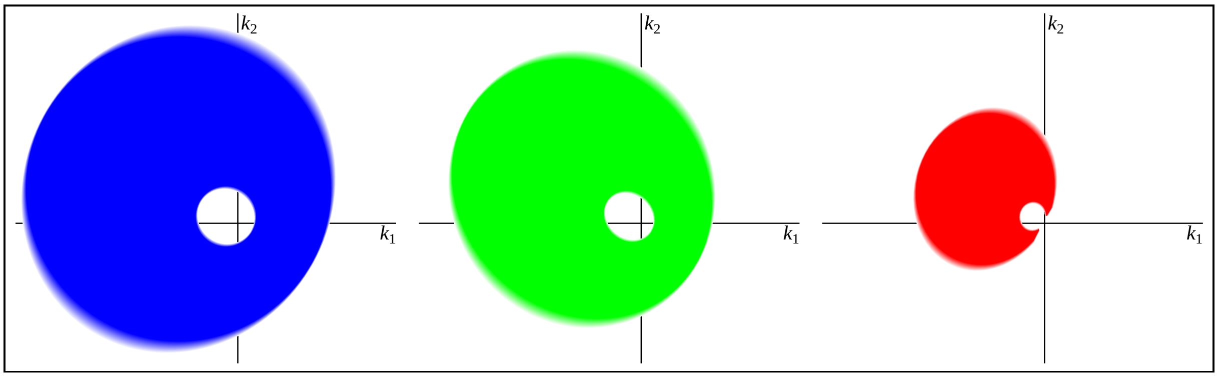

Figure 9. High–wavenumber domain, consisting of the structural wavenumbers generating narrow–band Gaussian packets for an incident P wave. Three colours correspond to three polarizations of the scattered wave. Note that different polarizations and different directions of the structural wavenumber vector $\mathbf{k}^\alpha$ are sensitive to different linear combinations (68) of perturbations of elastic moduli and density. When changing the source, the wavenumber domain of sensitivity "rotates" with the direction of the incident wavefield, and the reflectivity function (68) changes, allowing to resolve more elastic moduli.

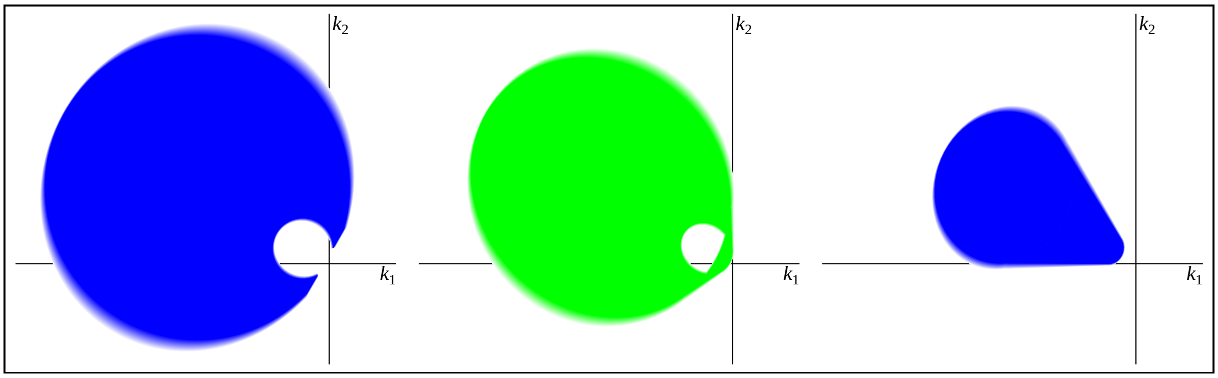

Figure 10. High–wavenumber domain, consisting of the structural wavenumbers generating narrow–band Gaussian packets for an incident slower S wave. Three colours correspond to three polarizations of the scattered wave. Analogous to Figure 9 which corresponds to an incident P wave. Note that the scattered waves are sensitive to other linear combinations (68) of perturbations of elastic moduli and density than the scattered waves corresponding to an incident P wave.

5.2. Broad–band scattering

If the deviation of $\mathbf{k}^{\alpha}$ from the tangent plane to $\mathcal{S}_{\mathbf{P}_{\omega_0}}$ at $\mathbf{k}^{\alpha}$ is small, or if $\mathbf{k}^{\alpha}$ is small, the beams are scattered in a broad frequency band. In this case, the incident wavefield can be decomposed into narrow–band Gabor signals using the Gabor transform. The scattered beams of each narrow–band component of the broad–band incident wavefield form a single space–time Gaussian packet. Gaussian packets of different prevailing frequencies propagate in different directions, forming a broad–band fan of narrow–band Gaussian packets. The existence and scattering angle of a Gaussian packet depends on the structural wavenumber vector $\mathbf{k}^{\alpha}$.

This is typical forward and narrow–angle scattering at low wavenumbers $|\mathbf{k}^{\alpha}|$, but occurs also for S to P wave scattering at high wavenumbers $|\mathbf{k}^{\alpha}|$. For a particular incident wave, there may be 2 different kinds of broad–band fans of scattered narrow–band Gaussian packets: one belonging to low wavenumbers $|\mathbf{k}^{\alpha}|$ ($\omega^0 = +\infty$), see Figures 11 and 13, the other belonging to $\mathbf{k}^{\alpha}$ from the conical surface tangent to the P–wave sheets of the wavenumber surfaces $\mathcal{S}_{\mathbf{P}_{\omega}}$ during S to P wave scattering (finite ω^0), see Figure 16. In a strongly anisotropic background, there may also occur a wide–angle broad–band S to S scattering with conversion from slow to fast S wave (see Figure 15), analogous to wide–angle broad–band S to P scattering.

We shall refer to the set of low wavenumber vectors $\mathbf{k}^{\alpha}$, causing forward or narrow–angle broad–band scattering without wave conversion, as the "low–wavenumber domain", see Figures 11 and 13. The scattering angle of the Gaussian packet, generated by a Gabor function belonging to the low–wavenumber domain, is inversely proportional to the prevailing frequency of the packet. The low–wavenumber domain is usually being recovered by travel–time tomography (see Figures 12 and 14) and wave–equation tomography.

Note that the union of low–wavenumber domains corresponding to different incident waves may overlap with the union of high–wavenumber domains corresponding to different incident waves.

Following Sections 5.3 to 5.6 are devoted to narrow–band scattering only. The equations should be generalized to broad–band scattering in future.

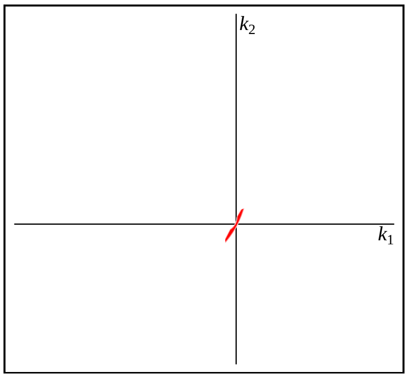

Figure 11. Low–wavenumber domain, consisting of the structural wavenumbers generating a broad–band scattered wavefield, for an incident P wave.

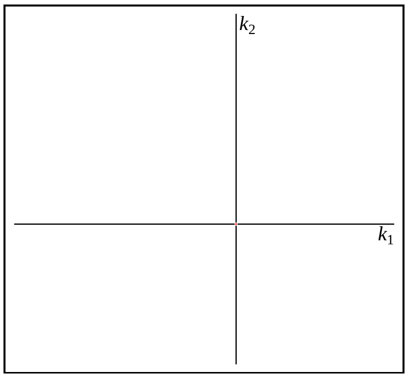

Figure 12. Ultralow–wavenumber domain, consisting of the structural wavenumbers resolved by travel–time tomography, for an incident P wave.

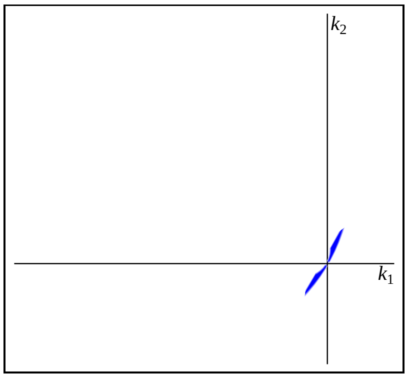

Figure 13. Low–wavenumber domain, consisting of the structural wavenumbers generating a broad–band scattered wavefield, for an incident slower S wave.

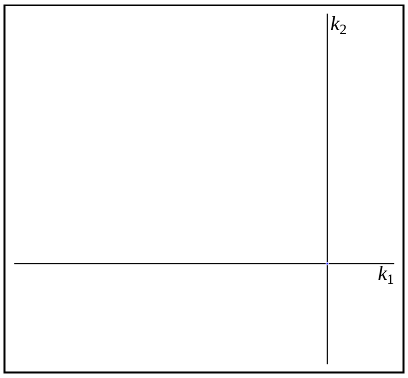

Figure 14. Ultralow–wavenumber domain, consisting of the structural wavenumbers resolved by travel–time tomography, for an incident slower S wave.

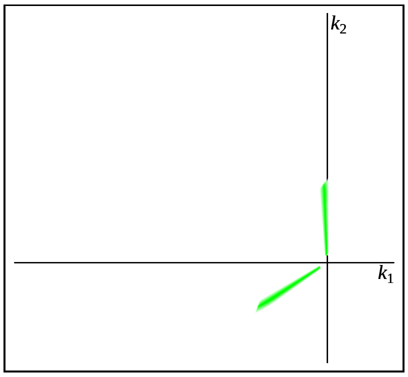

Figure 15. High–wavenumber domain, consisting of the structural wavenumbers generating a broad–band scattered wavefield, for an incident slower S wave and scattered faster S wave.

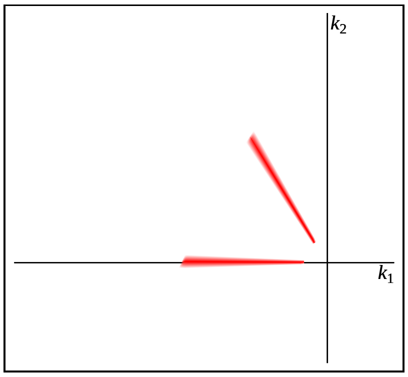

Figure 16. High–wavenumber domain, consisting of the structural wavenumbers generating a broad–band scattered wavefield, for an incident slower S wave and scattered P wave.

5.3. Fourier transform

Analytical signal $u_i^{\alpha(\mathrm{A})}(\mathbf{x},t)$ corresponding to the Gaussian packet scattered by Gabor function $g^\alpha(\mathbf{x})$ can be obtained by inverse Fourier transform (14) of the frequency–dependent Gaussian beam $\widehat{u}_i^\alpha(\mathbf{x},\omega)$,

$$u_i^{\alpha(\mathrm{A})}(\mathbf{x},t) = \frac{1}{\pi}\int\limits_0^{+\infty} \mathrm{d}\omega \exp(-\mathrm{i}\omega t)\,\widehat{u}_i^\alpha(\mathbf{x},\omega) \quad . \tag{211}$$

We insert (78) into (211),

$$u_i^{\alpha(\mathrm{A})}(\mathbf{x},t) = \frac{1}{\pi}\,e_i(\mathbf{x},\mathbf{x}^\alpha)\int\limits_0^{+\infty} \mathrm{d}\omega\;\widehat{a}(\mathbf{x},\omega)\,\exp\{\mathrm{i}\omega[T_\omega^\alpha(\mathbf{x})-t]\} \quad . \tag{212}$$

We assume a smooth frequency spectrum and approximate amplitude $\widehat{a}_i(\mathbf{x},\omega)$ by its value at prevailing frequency ω^0,

$$u_i^{\alpha(\mathrm{A})}(\mathbf{x},t) = \frac{1}{\pi}\,e_i(\mathbf{x},\mathbf{x}^\alpha)\,\widehat{a}(\mathbf{x},\omega^0)\int\limits_0^{+\infty} \mathrm{d}\omega \exp\{\mathrm{i}\omega[T_\omega^\alpha(\mathbf{x})-t]\} \quad . \tag{213}$$

We have thus neglected the frequency dependence of terms ω^2, $\widehat{A}(\mathbf{x}^\alpha,\omega)$ and $K_{ij}^\alpha - \mathrm{i}\omega\theta_{,ij}^{\alpha\prime\prime}$ in (79).

We insert relation (155) for $T_\omega^\alpha(\mathbf{x})$, and express the frequency dependence of exponential term $\mathrm{i}\omega[T_\omega^\alpha(\mathbf{x})-t]$ in (213) as

$$\mathrm{i}\omega[T_\omega^\alpha(\mathbf{x})-t] = \mathrm{i}\omega^0[T_{\omega^0}^\alpha(\mathbf{x})-t] + \mathrm{i}\Delta\omega[T_{\omega^0}^\alpha(\mathbf{x})-t] + \mathrm{i}\Delta x_K^{(q)} M_{K4}\Delta\omega + \tfrac{1}{2}\mathrm{i}(\omega)^{-1}M_{44}(\Delta\omega)^2 \;, \tag{214}$$

where $T_{\omega^0}^\alpha(\mathbf{x})$ is defined by equation (143). Within a sufficiently narrow frequency band, the frequency–dependent matrix $(\theta^{0\prime\prime}+\mathrm{i}\omega^{-1}K^\alpha)_{ij}^{-1}$, used to define M_{ij} in (143) and to define $\mathbf{M}_4$ and M_{44} in (214) may be approximated by their value at $\omega=\omega^0$. We also approximate ω^{-1} in the last term of equation (214) by $(\omega^0)^{-1}$. We then rearrange equation (214) as

$$\begin{aligned}\mathrm{i}\omega[T_\omega^\alpha(\mathbf{x})-t] \approx{}& \mathrm{i}\omega^0[T_{\omega^0}^\alpha(\mathbf{x})-t] + \tfrac{1}{2}\mathrm{i}(\omega^0)^{-1}M_{44}\{\Delta\omega + \omega^0[T_{\omega^0}^\alpha(\mathbf{x})-t+\Delta x_K^{(q)}M_{K4}]/M_{44}\}^2 \\ & -\tfrac{1}{2}\mathrm{i}\omega^0[T_{\omega^0}^\alpha(\mathbf{x})-t+\Delta x_K^{(q)}M_{K4}]^2/M_{44} \quad ,\end{aligned} \tag{215}$$

where all quantities at the right–hand side, except $\Delta\omega$, are approximated by their value at $\omega=\omega^0$.

Replacing integration variable $\mathrm{d}\omega$ in (213) by $\mathrm{d}\Delta\omega$ and calculating the integral analytically, we obtain Gaussian packet

$$\boxed{u_i^{\alpha(\mathrm{A})}(\mathbf{x},t) = e_i(\mathbf{x},\mathbf{x}^\alpha)\,a_{\mathbf{GP}}(\mathbf{x})\exp[\mathrm{i}\omega^0\,T_{\mathbf{GP}}^\alpha(\mathbf{x},t)] \quad ,} \tag{216}$$

where the vectorial amplitude of the scattered Gaussian packet is

$$a_{\mathbf{GP}}(\mathbf{x}) = \widehat{a}(\mathbf{x},\omega^0)\sqrt{\frac{2}{\pi}\frac{\mathrm{i}\omega^0}{M_{44}}} \quad , \tag{217}$$

and the complex–valued travel time of the scattered Gaussian packet is

$$T^\alpha_{\mathbf{GP}}(\mathbf{x},t) = T^\alpha_{\omega^0}(\mathbf{x}) - t - \tfrac{1}{2}[T^\alpha_{\omega^0}(\mathbf{x}) - t + \Delta x^{(q)}_K M_{K4}]^2/M_{44} \quad . \tag{218}$$

We approximate the second term $T^\alpha_{\omega^0}(\mathbf{x})$ in (218) by its linear Taylor expansion with respect to $\Delta x^{(q)}_i$,

$$T^\alpha_{\omega^0}(\mathbf{x}) \approx T^\alpha + \tau^0 + \tfrac{\mathrm{d}\tau}{\mathrm{d}q_3}\Delta x^{(q)}_3 \quad , \tag{219}$$

see (53) and (143). Then

$$\begin{aligned} T^\alpha_{\mathbf{GP}}(\mathbf{x},t) = {} & T^\alpha_{\omega^0}(\mathbf{x}) - t - \tfrac{1}{2}(M_{44})^{-1}(M_{K4}\Delta x^{(q)}_K)^2 \\ & + (M_{44})^{-1}M_{K4}\Delta x^{(q)}_K(t - T^\alpha - \tau^0 - \tfrac{\mathrm{d}\tau}{\mathrm{d}q_3}\Delta x^{(q)}_3) \\ & - \tfrac{1}{2}(M_{44})^{-1}[(\tfrac{\mathrm{d}\tau}{\mathrm{d}q_3})^2(\Delta x^{(q)}_3)^2 - 2\tfrac{\mathrm{d}\tau}{\mathrm{d}q_3}\Delta x^{(q)}_3(t - T^\alpha - \tau^0) + (t - T^\alpha - \tau^0)^2] \; . \end{aligned} \tag{220}$$

We insert (143) into (220) and obtain the complex–valued travel time of the Gaussian packet in the form

$$\begin{aligned} T^\alpha_{\mathbf{GP}}(\mathbf{x},t) = {} & T^\alpha + \tau^0 - t + \tfrac{\mathrm{d}\tau}{\mathrm{d}q_3}\Delta x^{(q)}_3 + \tfrac{1}{2}\Delta x^{(q)}_i M_{\mathbf{GP}\,ij}\Delta x^{(q)}_j \\ & + \Delta x^{(q)}_i M_{\mathbf{GP}\,i4}(t - T^\alpha - \tau^0) + \tfrac{1}{2}M_{\mathbf{GP}\,44}(t - T^\alpha - \tau^0)^2 \quad , \end{aligned} \tag{221}$$

where

$$M_{\mathbf{GP}\,KL} = M_{KL} - \frac{M_{K4}M_{L4}}{M_{44}} \quad , \tag{222}$$

$$M_{\mathbf{GP}\,K4} = \frac{M_{K4}}{M_{44}} \quad , \tag{223}$$

$$M_{\mathbf{GP}\,44} = -\frac{1}{M_{44}} \quad , \tag{224}$$

$$M_{\mathbf{GP}\,34} = -M_{\mathbf{GP}\,44}\tfrac{\mathrm{d}\tau}{\mathrm{d}q_3} \tag{225}$$

(Klimeš, 2004, eq. 68; Červený, Klimeš & Pšenčík, 2007, eq. 165), and

$$M_{\mathbf{GP}\,i3} = -M_{\mathbf{GP}\,i4}\tfrac{\mathrm{d}\tau}{\mathrm{d}q_3} + M_{i3} \tag{226}$$

(Klimeš, 2004, eqs. 67, 69; Červený, Klimeš & Pšenčík, 2007, eqs. 163, 164). Equations (222) and (223) in matrix notation read

$$\mathbf{M}_{\mathbf{GP}} = \mathbf{M} - \frac{\mathbf{M}_4\mathbf{M}_4^{\mathrm{T}}}{M_{44}} \tag{227}$$

and

$$\mathbf{M}_{\mathbf{GP}\,4} = \frac{\mathbf{M}_4}{M_{44}} \quad . \tag{228}$$

Note that the inverse relations to (227), (228), (224) and (217) read

$$\mathbf{M} = \mathbf{M}_{\mathbf{GP}} - \frac{\mathbf{M}_{\mathbf{GP}\,4}\mathbf{M}_{\mathbf{GP}\,4}^{\mathrm{T}}}{M_{\mathbf{GP}\,44}} \quad , \tag{229}$$

$$\mathbf{M}_4 = -\frac{\mathbf{M}_{\mathbf{GP}\,4}}{M_{\mathbf{GP}\,44}} \quad , \tag{230}$$

$$M_{44} = -\frac{1}{M_{\mathbf{GP}\,44}} \quad , \tag{231}$$

and

$$\widehat{a}(\mathbf{x},\omega^0) = a_{\mathbf{GP}}(\mathbf{x})\sqrt{\frac{\pi}{2}\frac{1}{-\mathrm{i}\omega^0 M_{\mathbf{GP}\,44}}} \quad . \tag{232}$$

5.4. Initial values of the scattered Gaussian packet

The initial values of the second–order travel–time derivatives (227), (228), (224) and of amplitude (217) at point $\mathbf{x}^\alpha$ are

$$\mathbf{M}^\alpha_{\mathbf{GP}} = \mathbf{M}^\alpha - (M^\alpha_{44})^{-1}\mathbf{M}^\alpha_4\mathbf{M}^{\alpha\,\mathrm{T}}_4 \quad , \tag{233}$$

$$\mathbf{M}^\alpha_{\mathbf{GP}\,4} = (M^\alpha_{44})^{-1}\mathbf{M}^\alpha_4 \quad , \tag{234}$$

$$M^\alpha_{\mathbf{GP}\,44} = -(M^\alpha_{44})^{-1} \quad , \tag{235}$$

and

$$a_{\mathbf{GP}}(\mathbf{x}^\alpha) = \widehat{a}(\mathbf{x}^\alpha,\omega^0)\sqrt{\frac{2}{\pi}\frac{\mathrm{i}\omega^0}{M^\alpha_{44}}} \quad . \tag{236}$$

Inserting (130), (146) and (153) into (233), we arrive at

$$\boxed{\mathbf{M}^\alpha_{\mathbf{GP}} = \mathbf{T}^{(q)} + \mathrm{i}\omega^{-1}\mathbf{K}^{(q)} - \frac{\mathbf{k}^{(q)}}{k_3^{(q)}}\,\mathbf{m}^\mathrm{T} - \mathbf{m}\left(\frac{\mathbf{k}^{(q)}}{k_3^{(q)}}\right)^\mathrm{T} + m\,\frac{\mathbf{k}^{(q)}}{k_3^{(q)}}\left(\frac{\mathbf{k}^{(q)}}{k_3^{(q)}}\right)^\mathrm{T} \quad ,} \tag{237}$$

where $\mathbf{m}$ is defined by (127) and m is defined by (128). Inserting (146) and (153) into (234), we arrive at

$$\boxed{\mathbf{M}^\alpha_{\mathbf{GP}\,4} = \frac{\omega^0}{k_3^{(q)}}\left(m\frac{\mathbf{k}^{(q)}}{k_3^{(q)}} - \mathbf{m}\right) \quad .} \tag{238}$$

Inserting (153) into (235), we arrive at

$$\boxed{M^\alpha_{\mathbf{GP}\,44} = \left(\frac{\omega^0}{k_3^{(q)}}\right)^2 m \quad .} \tag{239}$$

Inserting (153) and (163) into (236), we arrive at

$$a_{\mathbf{GP}}(\mathbf{x}^\alpha) = \mathrm{i}\omega^0\widehat{A}(\mathbf{x}^\alpha,\omega)\; r^\alpha(\mathbf{x})\;\tfrac{\mathrm{d}\tau}{\mathrm{d}q_3}(\mathbf{x}^\alpha)\;\frac{2\omega^0}{k_3^{(q)}} \quad . \tag{240}$$

Inserting (132), (99) and (81) into (240), we obtain

$$\boxed{a_{\mathbf{GP}}(\mathbf{x}^\alpha) = \mathrm{i}\omega^0\widehat{A}(\mathbf{x}^\alpha,\omega)\; r^\alpha(\mathbf{x})\;\frac{2}{1-P_iH^{,i}} \quad ,} \tag{241}$$

where P_i is the slowness vector of the incident wave and $H^{,i}$ is the ray–velocity vector of the scattered Gaussian packet at point $\mathbf{x}^\alpha$.

5.5. Evolution equations of the scattered Gaussian packet

We define matrices

$$\mathbf{Q}_{\mathrm{GP}} = \mathbf{Q}_1 + \mathbf{Q}_2 \mathbf{M}^{\alpha}_{\mathrm{GP}} \tag{242}$$

and

$$\mathbf{P}_{\mathrm{GP}} = \mathbf{P}_1 + \mathbf{P}_2 \mathbf{M}^{\alpha}_{\mathrm{GP}} \quad , \tag{243}$$

where $\mathbf{Q}_1$, $\mathbf{P}_1$, $\mathbf{Q}_2$ and $\mathbf{P}_2$ form paraxial ray propagator matrix (113). Parameters describing a Gaussian packet should obey relations

$$\boxed{\mathbf{M}_{\mathrm{GP}} = \mathbf{P}_{\mathrm{GP}} \mathbf{Q}^{-1}_{\mathrm{GP}}} \tag{244}$$

(Klimeš, 2004, eq. 50; Červený, Klimeš & Pšenčík, 2007, eq. 135),

$$\boxed{\mathbf{M}_{\mathrm{GP}\,4} = \mathbf{Q}^{-1\,\mathrm{T}}_{\mathrm{GP}} \mathbf{M}^{\alpha}_{\mathrm{GP}\,4}} \tag{245}$$

(Klimeš, 2004, eq. 74; Červený, Klimeš & Pšenčík, 2007, eq. 166),

$$\boxed{\mathbf{M}_{\mathrm{GP}\,3} = -\tfrac{\mathrm{d}\tau}{\mathrm{d}q_3} \mathbf{M}_{\mathrm{GP}\,4} + \mathbf{M}_3} \tag{246}$$

(Klimeš, 2004, eq. 67; Červený, Klimeš & Pšenčík, 2007, eq. 163), where $\mathbf{M}_3$ is defined by (110) and (112),

$$\boxed{M_{\mathrm{GP}\,44} = M^{\alpha}_{\mathrm{GP}\,44} - \mathbf{M}_{\mathrm{GP}\,4}{}^{\mathrm{T}} \mathbf{Q_2} \mathbf{M}^{\alpha}_{\mathrm{GP}\,4}} \tag{247}$$

(Klimeš, 2004, eq. 79),

$$\boxed{M_{\mathrm{GP}\,34} = -\tfrac{\mathrm{d}\tau}{\mathrm{d}q_3} M_{\mathrm{GP}\,44}} \tag{248}$$

(Klimeš, 2004, eq. 68; Červený, Klimeš & Pšenčík, 2007, eq. 165),

$$\boxed{M_{\mathrm{GP}\,33} = (\tfrac{\mathrm{d}\tau}{\mathrm{d}q_3})^2 M_{\mathrm{GP}\,44} + M_{33}} \tag{249}$$

(Klimeš, 2004, eq. 69; Červený, Klimeš & Pšenčík, 2007, eq. 164), where M_{33} is defined by (110) and (112), and

$$\boxed{a_{\mathrm{GP}}(\mathbf{x}) = R(\mathbf{x},\mathbf{x}^{\alpha}) \sqrt{\frac{\varrho(\mathbf{x}^{\alpha}) \frac{\mathrm{d}\tau}{\mathrm{d}q_3}(\mathbf{x}) h(\mathbf{x}^{\alpha})}{\varrho(\mathbf{x}) \frac{\mathrm{d}\tau}{\mathrm{d}q_3}(\mathbf{x}^{\alpha}) h(\mathbf{x})}} \, \frac{1}{\sqrt{\det[\mathbf{Q}_{\mathrm{GP}}(\mathbf{x},\mathbf{x}^{\alpha})]}} \, a_{\mathrm{GP}}(\mathbf{x}^{\alpha}) \quad .} \tag{250}$$

Term $\sqrt{\det[\mathbf{Q}_{\mathrm{GP}}(\mathbf{x},\mathbf{x}^{\alpha})]}$ is equal to 1 at $\mathbf{x} = \mathbf{x}^{\alpha}$, and then varies continuously along the ray.

5.6. Proof of the evolution equations

In Section 5.3, we derived the scattered Gaussian packets under the assumption of narrow–band scattering. In Section 5.4, we determined the initial conditions for these Gaussian packets, and in Section 5.5, we summarized the evolution equations which Gaussian packets should obey. We shall now prove that the equations derived in Section 5.3 are equivalent to the equations expressed Section 5.5

Equation (246) is equivalent to (226). Equation (248) coincides with (225). Equation (249) follows from (226) with (225). We now prove equations (244), (245), (247) and (250).

5.6.1. Equivalence of (227) and (244)

We shall convert equation (244) using previously derived equations into equation (227). Considering equation (142), equation (244) is equivalent to

$$\mathbf{Q}^{\mathrm{T}}(\mathbf{M}_{\mathrm{GP}} - \mathbf{M})\mathbf{Q}_{\mathrm{GP}} = \mathbf{Q}^{\mathrm{T}}\mathbf{P}_{\mathrm{GP}} - \mathbf{P}^{\mathrm{T}}\mathbf{Q}_{\mathrm{GP}} \quad . \tag{251}$$

Considering symplectic property

$$\mathbf{Q}^{\mathrm{T}}\mathbf{P}_{\mathrm{GP}} - \mathbf{P}^{\mathrm{T}}\mathbf{Q}_{\mathrm{GP}} = \mathbf{Q}^{\alpha\,\mathrm{T}}\mathbf{P}^{\alpha}_{\mathrm{GP}} - \mathbf{P}^{\alpha\,\mathrm{T}}\mathbf{Q}^{\alpha}_{\mathrm{GP}} \tag{252}$$

and definitions (140), (141), (242), (243), equation (251) is equivalent to

$$\mathbf{Q}^{\mathrm{T}}(\mathbf{M}_{\mathrm{GP}} - \mathbf{M})\mathbf{Q}_{\mathrm{GP}} = \mathbf{M}^{\alpha}_{\mathrm{GP}} - \mathbf{M}^{\alpha} \quad . \tag{253}$$

Considering equation (233), equation (253) is equivalent to

$$\mathbf{M}_{\mathrm{GP}} = \mathbf{M} - \mathbf{Q}^{-1\,\mathrm{T}}\mathbf{M}^{\alpha}_{4}\mathbf{M}^{\alpha\,\mathrm{T}}_{4}\mathbf{Q}^{-1}_{\mathrm{GP}}(M^{\alpha}_{44})^{-1} \quad . \tag{254}$$

Definitions (140) and (242) with relation (233) yield

$$\mathbf{Q}_{\mathrm{GP}}\mathbf{Q}^{-1} = \mathbf{1} - (M^{\alpha}_{44})^{-1}\mathbf{Q_2}\mathbf{M}^{\alpha}_{4}\mathbf{M}^{\alpha\,\mathrm{T}}_{4}\mathbf{Q}^{-1} \quad . \tag{255}$$

The inverse matrix is

$$\mathbf{Q}\mathbf{Q}^{-1}_{\mathrm{GP}} = \mathbf{1} - \frac{\mathbf{Q_2}\mathbf{M}^{\alpha}_{4}\mathbf{M}^{\alpha\,\mathrm{T}}_{4}\mathbf{Q}^{-1}}{\mathbf{M}^{\alpha\,\mathrm{T}}_{4}\mathbf{Q}^{-1}\mathbf{Q_2}\mathbf{M}^{\alpha}_{4} - M^{\alpha}_{44}} \quad . \tag{256}$$

Considering equation (256), equation (254) is equivalent to

$$\mathbf{M}_{\mathrm{GP}} = \mathbf{M} - \mathbf{Q}^{-1\,\mathrm{T}}\mathbf{M}^{\alpha}_{4}\mathbf{M}^{\alpha\,\mathrm{T}}_{4}\mathbf{Q}^{-1}(M^{\alpha}_{44})^{-1}\left[1 - \frac{\mathbf{M}^{\alpha\,\mathrm{T}}_{4}\mathbf{Q}^{-1}\mathbf{Q_2}\mathbf{M}^{\alpha}_{4}}{\mathbf{M}^{\alpha\,\mathrm{T}}_{4}\mathbf{Q}^{-1}\mathbf{Q_2}\mathbf{M}^{\alpha}_{4} - M^{\alpha}_{44}}\right] , \tag{257}$$

which is equivalent to

$$\mathbf{M}_{\mathrm{GP}} = \mathbf{M} + \frac{\mathbf{Q}^{-1\,\mathrm{T}}\mathbf{M}^{\alpha}_{4}\mathbf{M}^{\alpha\,\mathrm{T}}_{4}\mathbf{Q}^{-1}}{\mathbf{M}^{\alpha\,\mathrm{T}}_{4}\mathbf{Q}^{-1}\mathbf{Q_2}\mathbf{M}^{\alpha}_{4} - M^{\alpha}_{44}} \quad . \tag{258}$$

Considering equations (150) and (154), equation (258) is equivalent to equation (227).

5.6.2. Equivalence of (228) and (245)

We shall convert equation (228) into equation (245). Inserting equations (150) and (154) into equation (228), we obtain

$$\mathbf{M}_{\mathrm{GP}\,4} = \frac{\mathbf{Q}^{-1\,\mathrm{T}}\mathbf{M}_4^\alpha}{M_{44}^\alpha - \mathbf{M}_4^{\alpha\,\mathrm{T}}\mathbf{Q}^{-1}\mathbf{Q_2}\mathbf{M}_4^\alpha} \quad . \tag{259}$$

We multiply equation (259) by equation

$$\mathbf{Q}_{\mathrm{GP}}^{\mathrm{T}} = \mathbf{Q}^{\mathrm{T}} - (M_{44}^\alpha)^{-1}\mathbf{M}_4^\alpha\mathbf{M}_4^{\alpha\,\mathrm{T}}\mathbf{Q_2}^{\mathrm{T}} \quad . \tag{260}$$

following from (255) and obtain

$$\mathbf{Q}_{\mathrm{GP}}^{\mathrm{T}}\mathbf{M}_{\mathrm{GP}\,4} = \frac{\mathbf{M}_4^\alpha - (M_{44}^\alpha)^{-1}\mathbf{M}_4^\alpha\mathbf{M}_4^{\alpha\,\mathrm{T}}\mathbf{Q_2}^{\mathrm{T}}\mathbf{Q}^{-1\,\mathrm{T}}\mathbf{M}_4^\alpha}{M_{44}^\alpha - \mathbf{M}_4^{\alpha\,\mathrm{T}}\mathbf{Q}^{-1}\mathbf{Q_2}\mathbf{M}_4^\alpha} \quad . \tag{261}$$

It follows from equation (140) and from the symplecticity of the paraxial–ray propagator matrix (113) that matrix $\mathbf{Q}^{-1}\mathbf{Q_2}$ is symmetric. Equation (261) then reads

$$\mathbf{Q}_{\mathrm{GP}}^{\mathrm{T}}\mathbf{M}_{\mathrm{GP}\,4} = (M_{44}^\alpha)^{-1}\mathbf{M}_4^\alpha \quad , \tag{262}$$

which is equivalent to equation (245) with (234).

5.6.3. Equivalence of (224) and (247)

We shall convert equation (224) into equation (247). Inserting equation (154) into equation (224), we obtain

$$M_{\mathrm{GP}\,44} = \frac{1}{\mathbf{M}_4^{\alpha\,\mathrm{T}}\mathbf{Q}^{-1}\mathbf{Q_2}\mathbf{M}_4^\alpha - M_{44}^\alpha} \quad . \tag{263}$$

Subtracting equation (235), we arrive at

$$M_{\mathrm{GP}\,44} - M_{\mathrm{GP}\,44}^\alpha = (M_{44}^\alpha)^{-1}\frac{\mathbf{M}_4^{\alpha\,\mathrm{T}}\mathbf{Q}^{-1}\mathbf{Q_2}\mathbf{M}_4^\alpha}{\mathbf{M}_4^{\alpha\,\mathrm{T}}\mathbf{Q}^{-1}\mathbf{Q_2}\mathbf{M}_4^\alpha - M_{44}^\alpha} \quad . \tag{264}$$

Considering equations (234) and (259), equation (264) is equivalent to equation (247).

5.6.4. Equivalence of (217) and (250)

We shall convert equation (217) into equation (250). Equation (255) yields

$$\frac{\det(\mathbf{Q}_{\mathrm{GP}})}{\det(\mathbf{Q})} = 1 - (M_{44}^\alpha)^{-1}\mathbf{M}_4^{\alpha\,\mathrm{T}}\mathbf{Q}^{-1}\mathbf{Q_2}\mathbf{M}_4^\alpha \quad . \tag{265}$$

Considering (263),

$$\frac{\det(\mathbf{Q}_{\mathrm{GP}})}{\det(\mathbf{Q})} = -(M_{44}^\alpha M_{\mathrm{GP}\,44})^{-1} \quad . \tag{266}$$

Inserting (224),

$$M_{44} = M_{44}^\alpha\,\frac{\det(\mathbf{Q}_{\mathrm{GP}})}{\det(\mathbf{Q})} \quad . \tag{267}$$

Equation (217) with (267) reads

$$a_{\mathrm{GP}}(\mathbf{x}) = \widehat{a}(\mathbf{x},\omega^0)\sqrt{\frac{\det(\mathbf{Q})}{\det(\mathbf{Q}_{\mathrm{GP}})}}\sqrt{\frac{2}{\pi}\,\frac{\mathrm{i}\omega^0}{M_{44}^\alpha}} \quad . \tag{268}$$

Considering equations (164) and (236), equation (268) is equivalent to equation (250).

6. Limited aperture

In geophysics, the aperture covered by the receivers is usually limited (e.g., to an area on the Earth surface). Then only a fraction of scattered time–harmonic Gaussian beams is registered (compare Figures 7 and 17). Consequently, only the time–domain waves scattered by Gabor functions corresponding to the wavenumber vectors from the cones covered by the aperture are registered (compare Figures 9 and 18). The lost information on the on the corresponding linear combination (68) of elastic moduli usually cannot be recovered without additional a priori assumptions.

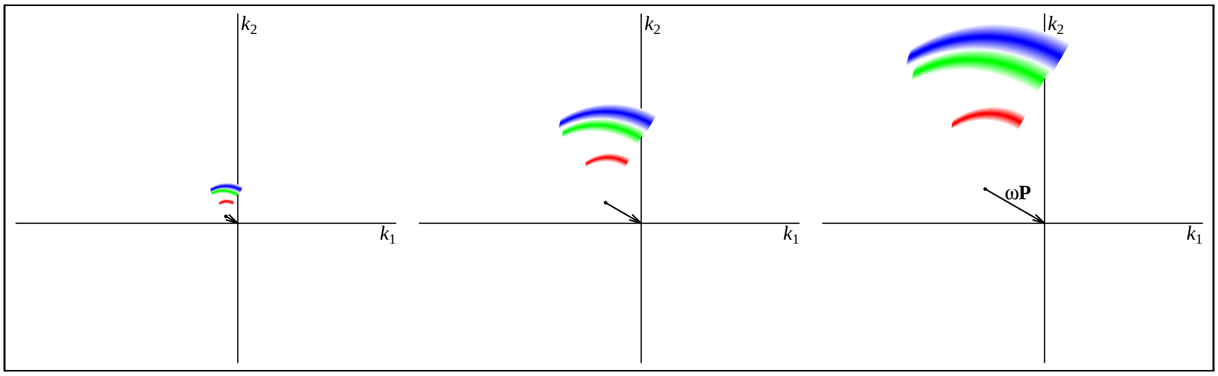

Figure 17. Scattering in the frequency domain — sensitivity of scattered Gaussian beams to structural wavenumbers at various positive frequencies ω for limited aperture. Compare to Figure 7.

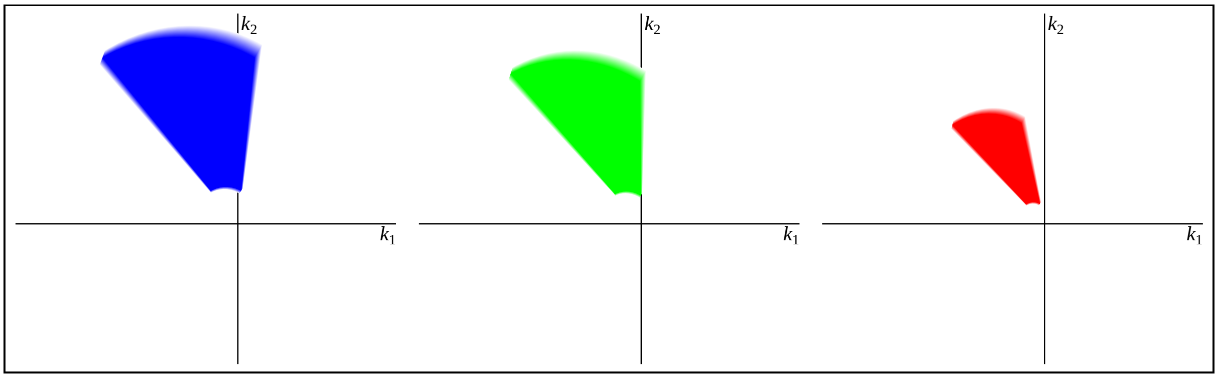

Figure 18. Scattering in the time domain — wavenumbers affecting the wavefield scattered within a limited aperture. Compare to Figure 9.

7. True–amplitude migrations

The derived approximate solution of the forward scattering problem may be utilized in designing the migration algorithm based on true linearized inversion of the complete set of seismograms recorded for all shots. The algorithm should be composed of the following steps:

(a) The migrated section is assumed to be decomposed into Gabor functions $g^{\alpha}(\mathbf{x})$ in form (3). The relation between the shape (4) of Gabor functions and the shape of scattered Gaussian packets should be employed to optimize the shape of Gabor functions. See the note in Section 7.1.

(b) For each source, the waves scattered by individual Gabor functions and arriving to the receiver array are calculated. These waves may approximately be composed of Gaussian packets according to this paper.

(c) The approximate linearized relation between factors c^{α}_{ijkl} and ϱ^{α} of the Gabor functions and the wavefield obtained in step (b) may be used to estimate these factors by a regularized least–square inversion.

7.1. Optimization of the Gabor representation

At each point $\mathbf{x}^{\alpha}$, we consider all source–receiver pairs and all corresponding combinations of elementary waves. For each combination of elementary waves from the source and from the receiver, we obtain a set of structural wavenumbers $\mathbf{k}^{\alpha}$ with corresponding frequencies ω from equation (81). For each $\mathbf{k}^{\alpha}$ and corresponding frequency ω, the shape of the scattered Gaussian packet depends on initial parameters $\mathbf{M}^{\alpha}_{\mathbf{GP}}$, $\mathbf{M}^{\alpha}_{\mathbf{GP}\,4}$ and $M^{\alpha}_{\mathbf{GP}\,44}$ through equations (244)–(249). Six initial parameters $\mathbf{M}^{\alpha}_{\mathbf{GP}}$, $\mathbf{M}^{\alpha}_{\mathbf{GP}\,4}$ and $M^{\alpha}_{\mathbf{GP}\,44}$ linearly depend on six independent components of symmetric 3×3 matrix $\mathbf{K}^{\alpha}$ through equations (237)–(239) with (127) and (128).

It would be nice to find a way how to optimize the shape of the scattered Gaussian packets by a proper selection of $\mathbf{K}^{\alpha}$ in dependence on $\mathbf{x}^{\alpha}$ and $\mathbf{k}^{\alpha}$.

8. Final remark

The derived correspondence between the perturbations of the structure and the recorded wavefield may play a decisive role in understanding the information on geological structures carried by seismic wavefields, in understanding the physical meaning of velocity macro models, and in interpretation of seismic data from forward to wide–angle scattering. It may allow us to understand the physical meaning and resolution of migrated images, and to estimate mispositioning and fuzziness of structural details due to inaccuracies in the velocity macro model.

Acknowledgements

The research has been supported by the Grant Agency of the Czech Republic under Contracts 205/01/0927, 205/04/1104 and 205/07/0032, by the Ministry of Education of the Czech Republic within research project MSM0021620860, and by the members of the consortium "Seismic Waves in Complex 3–D Structures" (see "http://sw3d.mff.cuni.cz").

References

Červený, V. (2001): *Seismic Ray Theory.* Cambridge Univ. Press, Cambridge.

Červený, V., Klimeš, L. & Pšenčík, I. (1984): Paraxial ray approximation in the computation of seismic wavefields in inhomogeneous media. *Geophys. J. R. astr. Soc.*, **79**, 89–104.

Červený, V., Klimeš, L. & Pšenčík, I. (2007): Seismic ray method: Recent developments. *Advances in Geophysics*, **48**, 1–126.

Klimeš, L. (1994): Transformations for dynamic ray tracing in anisotropic media. *Wave Motion*, **20**, 261–272.

Klimeš, L. (2004): Gaussian packets in smooth isotropic media. In: *Seismic Waves in Complex 3-D Structures, Report 14*, pp. 43–54, Dep. Geophys., Charles Univ., Prague, online at "http://sw3d.mff.cuni.cz".